IOWA STATE UNIVERSITY
Digital Repository

Retrospective Theses and Dissertations

Iowa State University Capstones, Theses and Dissertations

1997

Nonlinear control design for stressed power systems using normal forms of vector fields

Gilsoo Jang
Iowa State University

Follow this and additional works at: https://lib.dr.iastate.edu/rtd

Part of the Electrical and Electronics Commons, and the Oil, Gas, and Energy Commons

INFORMATION TO USERS

Nonlinear control design for stressed power systems

using normal forms of vector fields

by

Gilsoo Jang

A dissertation submitted to the graduate faculty

in partial fulfillment of the requirements for the degree of

DOCTOR OF PHILOSOPHY

Major: Electrical Engineering (Electric Power)

Major Professor: Dr. Vijay Vittal

Iowa State University

Ames, Iowa

1997

Graduate College
Iowa State University

This is to certify that the Doctoral dissertation of

Gilsoo Jang

has met the dissertation requirements of Iowa State University

Major Professor

For the Major Program

For the Graduate College

TABLE OF CONTENTS

LIST OF TABLES

LIST OF FIGURES

ACKNOWLEDGMENTS

I would like to thank my advisor, Dr. Vijay Vittal for his constant guidance and support throughout this work. His professional enthusiasm was of immense help during the course of this endeavor.

I would also like to thank Dr. G. B. Sheble, Dr. J. D. McCalley, Dr. M. Khamash, and Dr. D. Mirkovic for their valuable comments on this work and for serving on my committee. I am especially thankful to Dr. A. A. Fouad, Dr. Y. Ni, and Dr. W. Kliemann for their great help and encouragement.

I really appreciate the warm encouragement and advice given to me by Dr. Sae-Hyuk Kwon.

My sincere thanks to Byongjun Lee, Swapan Saha, Agustin Irizarry-Rivera, Charles Richter, Sundar Rajan, Manos Obessis, and Charles Pawloski for their friendship and assistance. Thanks are also due to all my friends at Iowa State University and those in Korea for the wonderful times we shared together.

I have no words that can do justice in expressing what my parents have meant to me from the time I was born. I would like to thank my mother-in-law and father-in-law for their unconditional support and encouragement. To my lovely wife, Eunjoo and to my son, Moon-Hyuk, I offer a sincere 'thank you' from the depths of my heart.

1 INTRODUCTION

Since the commercial use of electricity in the late 1870s, a major portion of the energy needs of modern society has been met by electrical energy. The function of an electric power system is to convert energy from one of the naturally available forms to the electrical form and to transport it to the points of consumption. The advantage of the electrical form of energy is that it can be transported and controlled with relative ease and with a high degree of efficiency and reliability. A properly designed and operated power system should, therefore, meet the following fundamental requirements (see chapter 1 of [1]):

- *The system must be able to meet the continually changing load demand for active and reactive power. Unlike other types of energy, electricity cannot be conveniently stored in sufficient quantities. Therefore, adequate "spinning" reserve of active and reactive power should be maintained and appropriately controlled at all times.*

- *The system should supply energy at minimum cost and with minimum ecological impact.*

- *The "quality" of power supply must meet certain minimum standards with regard to the following factors: constancy of frequency, constancy of voltage, and level of reliability.*

Several levels of controls involving a complex array of devices are used to meet the above requirements. These are depicted in Figure 1.1 which identifies the various sub-
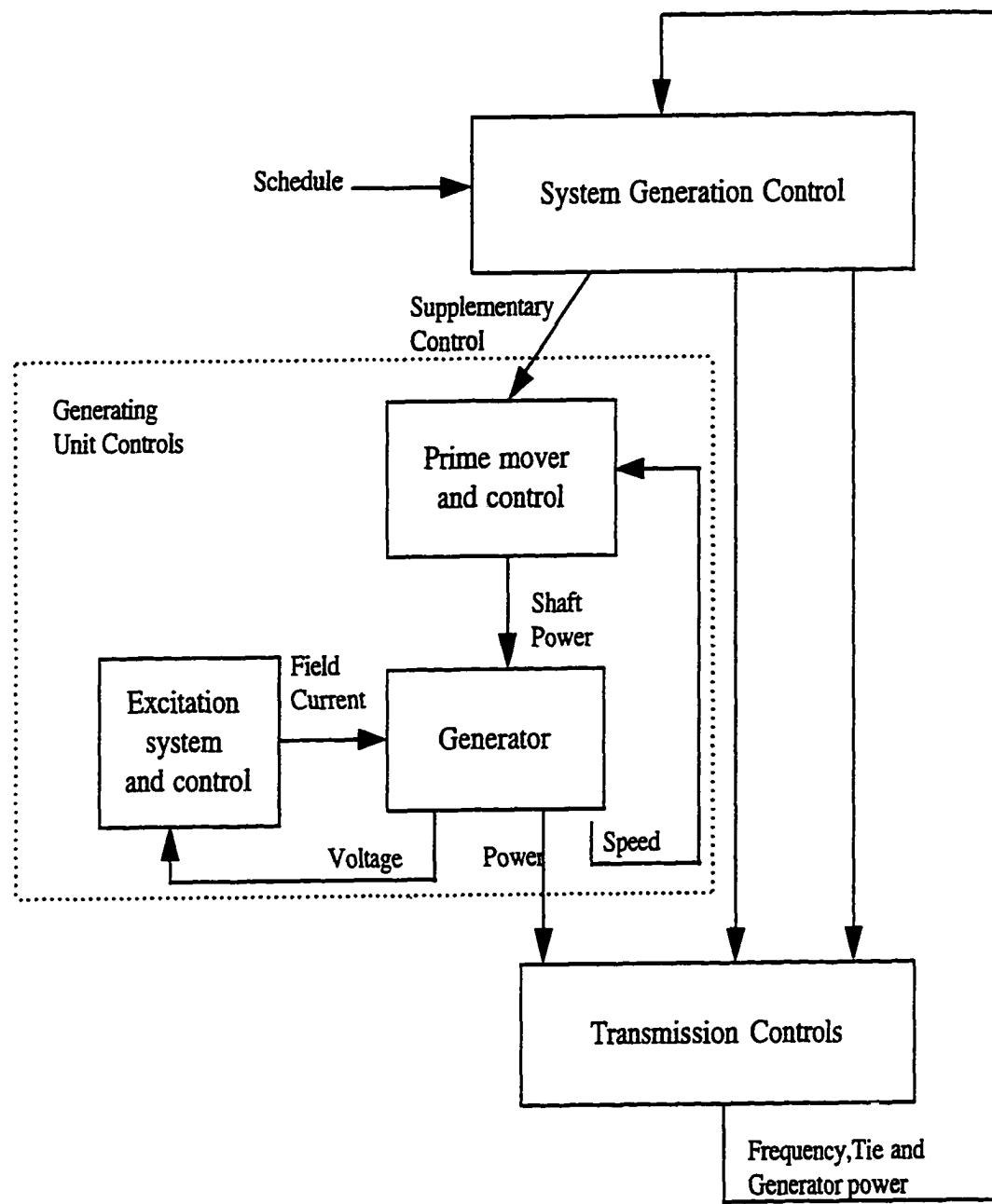
Figure 1.1   Subsystems of a power system and associated controls [1]

systems of a power system and the associated controls. In this overall structure, there are controllers operating directly on individual system elements. In a generating unit these consist of prime mover controls and excitation controls. The primary purpose of the system-generation control is to balance the total system generation against system load and losses so that the desired frequency and power interchange with neighboring systems is maintained. The transmission controls include power and voltage control devices and the controls described above contribute to the satisfactory operation of the power system by maintaining system voltages and frequency and other system variables within their acceptable limits. They also have a profound effect on the dynamic performance of the power system and on its ability to cope with disturbances. Major system failures are rarely the result of a single catastrophic disturbance causing collapse of an apparently secure system. Such failures are usually brought about by a combination of circumstances that stress the network beyond its capability.

1.1 Motivation for This Work

Electric power systems have become more complex and the operating characteristics of many power networks around the world have been changing considerably [2]:

- *Economic constraints associated with the price of energy production and capital investment made it attractive to transfer massive amounts of energy across utility borders. Now, more than 40% of the power generated by major utilities is sold to other utilities. Moreover, power transfer among utilities have more than doubled since 1971.*

- *Investments in transmission seems to be the hardest to justify. Almost every electric utility has experienced the difficulties of getting new transmission facilities approved and built, resulting in heavier loading of existing transmission. In some regions, the transmission is now fully loaded 95% of the time.*

- *The figures are not expected to be any better in the near future. Load growth is outpacing expansion.*

Therefore, available transmission and generation is highly utilized, with large amounts of power interchanged among companies and geographical regions. The stressed nature of power networks, described above, has an impact on the system dynamic behavior. Large stressed interconnected power systems exhibit complicated dynamic behavior when subjected to disturbances. This nonlinear complex behavior is not well analyzed with present tools, and a complete theoretical analysis of this is not feasible in large systems. However while a disturbance excites numerous modes of oscillation, only a few of these modes are of primary interest to the system designer. These include the poorly damped, low frequency interarea modes, in which generators that are geographically far away from each other participate, and control modes that represent the influence of the controllers on the system. In particular, excitation control is called upon to increase the damping of poorly damped inertial modes. Utilities have relied on high initial response excitation systems as an effective control of voltage and enhancement of system stability. Adequate system dynamic performance now depends on proper performance of controls [3]. In large systems, the design of controllers usually follows from a linear systems analysis, neglecting the possible nonlinear interaction between modes. The control design based on a linear approach performs suitably for certain operating conditions. However, power systems are inherently nonlinear and can operate over a wide range of conditions. With stressed conditions, the interarea mode phenomenon may occur and control performance can be altered by possible unfavorable *nonlinear modal interaction* among the power system. Such nonlinearities have undesirable effects, and control systems have to properly compensate them. Therefore, it is important to understand the nature of these nonlinear modal interactions and incorporate them in the analysis and design procedure. Also, these system characteristics call for improved analysis tools and

control design technique. This dissertation deals with these issues to develop a procedure to design controls incorporating the nonlinear information.

1.2 Problem Statement

The poorly damped, low frequency interarea modes play a crucial role in power system dynamic behavior, and controls are tuned to provide enough damping. If these modes interact with other modes nonlinearly, then the modal interaction may affect the control performance with respect to the crucial modes and control systems need to compensate such nonlinearities.

The objective of this work is to understand the effect of nonlinear modal interaction on control performance and to develop a procedure to determine the optimal controller setting. In this work normal forms of vector fields are used to provide the information regarding the nonlinear modal interaction. In addition the linear and nonlinear sensitivity techniques are developed and used to supplement control design.

1.3 Thesis Outline

The organization of the material is as follows: This introduction gives a motivation and objective of the research work. After this introductory chapter, a literature review provides a concise record of the source material for this work and general summary of the conventional linear gain tuning method. Chapter 3 presents the power system model used. In chapter 4, the general theory of eigenanalysis and normal forms is applied to the power system model described in chapter 3. Nonlinear modal interactions and mode-machine relationships are also addressed. Chapter 5 describes the sensitivity analysis which consists of sensitivity of the eigenvalue, eigenvector and normal form transformation coefficient. Chapter 6 presents the proposed control tuning procedure. Numerical results of the application of these techniques to a stressed power system are

presented in chapter 7. Chapter 8 provides conclusions, and the details of the derivation of the initial conditions, a sample program which makes use of parallel computing, and more data of the test system are found in the appendices.

2 LITERATURE REVIEW

2.1 Analysis of Stressed Power Systems

Oscillations associated with groups of generators, or groups of plants, are called interarea modes and are complex to study, and to control. Kundur, et.al. [4, 5] have presented the nature of interarea oscillation which is a characteristic of stressed power systems in the western United States using linear analysis techniques. In this study, both small signal and transient stability analyses are used to determine the characteristics of the system. Vittal, Bahtia, and Fouad [6] reported on the correlation between interarea modes and the size of the 2nd order terms in the series approximation of system's differential equations. Tamura, Yorino, and Yoo, et. al. [7, 8, 9] discussed auto-parametric resonance in the study of power system dynamic behavior. They described conditions for this type of resonance in the system's nonlinear oscillations and considered stressed system conditions.

Several analytical tools for studying power system dynamic performance have been presented. Time domain simulation is a well-known and widely accepted means for studying the nonlinear transient behavior of power system [4]. In the time domain simulation method, nonlinear differential and algebraic equations are used for modeling the power system, and these nonlinear equations are solved by an iterative step-by-step procedure to evaluate the system performance for various operating conditions, system configurations etc. This provides a detailed picture of the system's performance for specific conditions within the system. The disadvantages of this method are that the speed

of calculation is slow and this method can only tell us whether the system is stable or not, but can not provide qualitative information of the system's dynamic performance and sensitivity to system parameters. Direct methods based on the Lyapunov's theory, such as the transient energy function (TEF) method [10] are being used and further developed to analyze system performance and stability quantitatively. However, the information from TEF method is not enough to analyze the nature of the nonlinear interaction. The eigenanalysis for system dynamic performance has been widely used [3]. Agrawal, Anderson and Van Ness [11] used eigenanalysis for analyzing SSR (SubSynchronous Resonance). Another paper [12] describes eigenanalysis of second harmonic resonance related to a back-to-back dc links and associated static var compensators. Two papers [13, 14] describe more novel methods for examining one or more modes of very high order systems directly. They used the dynamic equivalencing and SMA (Selective Modal Analysis) to reduce the dynamic order of the system for eigenanalysis calculations. Despite several advantages of eigenanalysis, this is not suitable for analysis of nonlinear modal interaction since eigenanalysis is based on the linearized system and modes are decoupled in the analysis. The use of normal forms of vector fields is a well known mathematical tool for dynamical system analysis. It was presented by Poincare in his dissertation. Arrowsmith and Place [15], Arnold [16], and Ruelle [17] gave basic introductions to the Lie derivative-based method. A series of papers by the authors [18, 19, 20] shows that 2nd order nonlinear modal interaction obtained via normal forms of the system dynamics, allows insight into the nonlinear behavior of a power system (including AC/DC systems) and can be used to predict interarea separation [21]. For controlled power systems, [18] shows, by analyzing a four generator test system [1], that 2nd order nonlinear interactions between low frequency inertial modes and control modes are crucial to understand the dynamic behavior of these systems.

2.2 Excitation Control

The basic function of an excitation system is to provide direct current to the synchronous machine field winding. In addition, the excitation system performs control and protective functions essential to the satisfactory performance of the power system by controlling the field voltage and thereby the field current. Figure 2.1 shows the functional block diagram of a typical excitation control system for a large synchronous generator. The following is a brief description of the various subsystems identified in the figure (see chapter 8 of [1]).

- Exciter provides dc power to the synchronous machine field winding, constituting the power stage of the excitation system.

- Regulator processes and amplifies input control signals to a level and form appropriate for control of the exciter. This includes both regulating and excitation system stabilizing functions.

- Terminal voltage transducer and load compensator senses generator terminal voltage, rectifies and filters it to a dc quantity, and compares it with a reference which represents the desired terminal voltage.

- Power system stabilizer provides an additional input signal to the regulator to damp power system oscillations. Some commonly used signals are rotor speed deviation, accelerating power, and frequency deviation.

- Limiters and protective circuits include a wide array of control and protective functions which ensure that the capability limits of the exciter and synchronous generator are not exceeded.

The basic requirement is that the excitation system supply and automatically adjust the field current of the synchronous generator to maintain the terminal voltage as
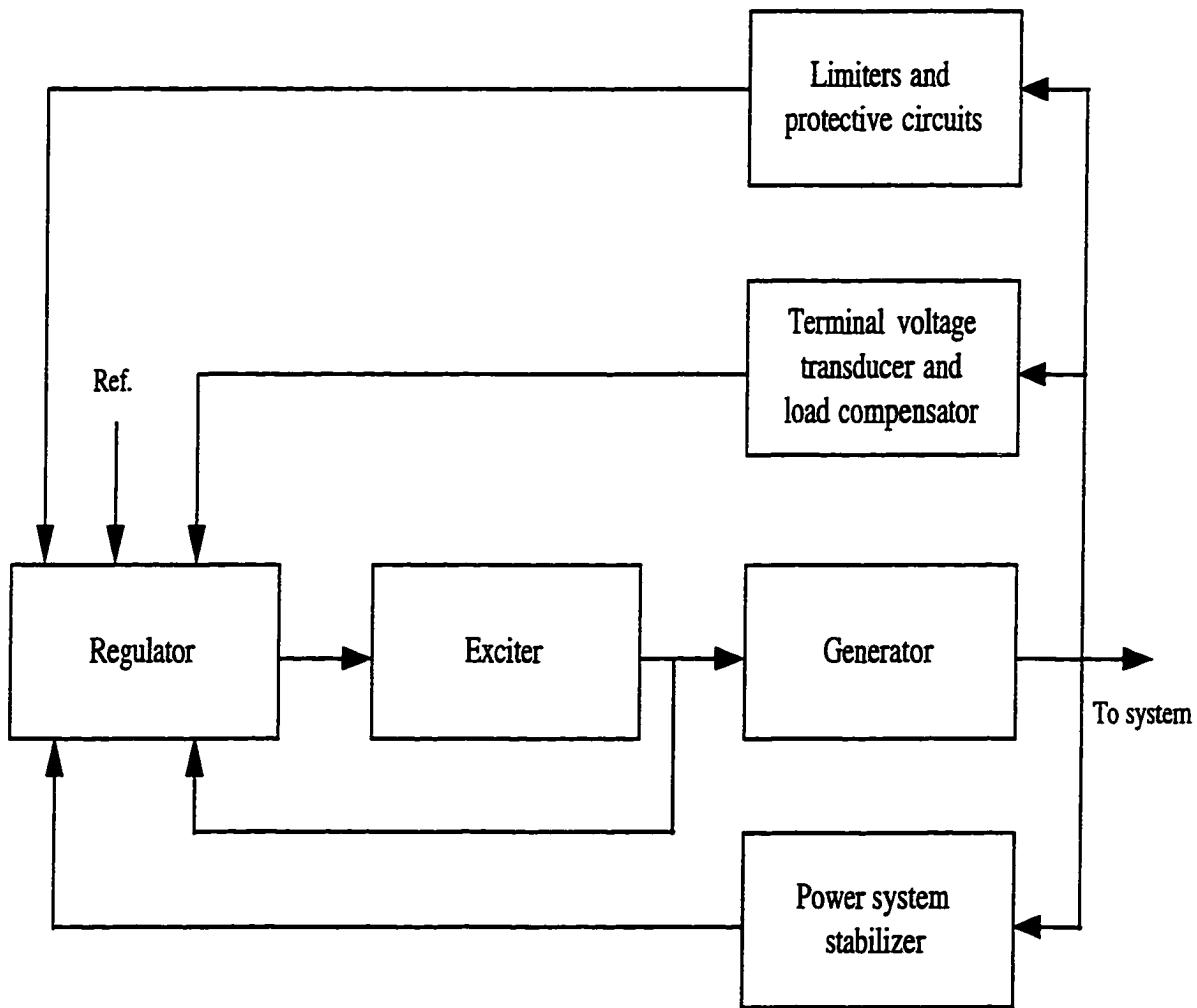
Figure 2.1   Functional block diagram of a synchronous generator excitation
control system [1]

the output varies within the *continuous capability* of the generator. In addition, the excitation system must be able to respond to transient disturbances with field forcing consistent with the generator instantaneous and short-term capabilities. To ensure the best utilization of the excitation system, it should be capable of meeting the system needs by taking full advantage of the generator's short-term capabilities without exceeding their limits.

The role of the excitation control systems in enhancing power system performance has been growing continually. In particular, the effects of the excitation systems on synchronous machine stability are widely investigated [22]. Physical systems including power systems are inherently nonlinear. Thus, all control systems are nonlinear to a certain extent. Nonlinearities may occur in any part of the system, and thus make it a nonlinear system. Usually, such nonlinearities have undesirable effects, and control systems have to properly compensate for them. Therefore we need a way to characterize and reduce the nonlinearities of power systems.

2.3 Linear Gain Tuning Method

Linear gain tuning algorithms adhere roughly to the following procedure: The critical (low frequency interarea) inertial modes with poor damping are identified. For the corresponding eigenvalues the sensitivity with respect to the exciter gains is computed. The exciter gain is shifted so that the real part of the critical eigenvalues becomes more negative. As a measure of the appropriate shift the linear approximation of the eigenvalues as functions of the exciter gains is used. The linear approximation can be computed from the eigenvalue and from its sensitivity. A technique based on the linear analysis of the system neglects potentially important terms in the system response. Therefore, it cannot always predict system behavior correctly (see [21] for e.g., analysis of system separation). Furthermore, such a technique does not always provide the mechanism by

which control settings influence the inertial modes as we will see below. The choice of the most influential exciter and of the amount of gain shifting may lead to inappropriate settings for system dynamic performance, when based on linear analysis alone. Finally, optimal gain values for the linear system and for the nonlinear system may be different, due to differences in the linear and the nonlinear response behavior. Therefore we propose a technique based on 2nd order normal forms.

3 POWER SYSTEM MODELS

In this chapter the power system model used in this dissertation is presented.

3.1 Generator Modeling

In this section simplified models of the generator are discussed. In power system dynamics study the response of a large number of synchronous machines to a given disturbance is investigated. The complete mathematical description of the system would be very complicated unless some simplifications were used. Often only a few machines are modeled in detail while others are described by simpler models.

In this work, we used two kinds of generator models which are the two-axis model and the classical model (see chapter 2 and 4 of [23]). We assume that in an n-generator system there are m generators represented by the two-axis model and equipped with exciters, the remaining n-m generators are presented by the classical model.

3.1.1 Classical Model

The classical model is based on the following assumptions:

1. Mechanical power input is constant.

2. Damping or asynchronous power is negligible.

3. Constant-voltage-behind-transient-reactance model for the synchronous machines is valid.

4. The mechanical rotor angle of a machine coincides with the angle of the voltage behind the transient reactance.

The equations of motion are given by

$$M_i \dot{\omega}_i = P_i - P_{ei} \tag{3.1}$$

$$\dot{\delta}_i = \omega_i - \omega_S \qquad i = m+1, m+2, ..., n$$

where,

$$P_i = P_{mi} - E_i^2 G_{ii}$$

$$P_{ei} = \sum_{j=1, j \neq i}^{n} [C_{ij} \sin(\delta_i - \delta_j) + D_{ij} \cos(\delta_i - \delta_j)]$$

$$C_{ij} = E_i E_j B_{ij}$$

$$D_{ij} = E_i E_j G_{ij}$$

and

E_i: internal bus voltage of generator i

M_i: inertia constant of generator i

P_{mi}: mechanical power input of generator i

G_{ii}: driving point conductance of node i

$G_{ij} + jB_{ij}$: the transfer admittance in the system reduced to the internal node between generators i and j

ω_i: rotor speed of generator i (with respect to synchronous frame)

ω_S: synchronous speed

δ_i: rotor angle of generator i

This model is used to represent the generators without excitation control in this work.

3.1.2 Two-axis Model

Generators with excitation control are described by the two-axis model (see chapter 4 of [23]) in this work. In the two-axis model the transient effects are accounted for and the following assumptions are required.

1. In the stator voltage equations the variation of flux linkages of d-q axes are negligible compare to the speed voltage terms.

2. $\omega \cong \omega_R = 1$ p.u.

The resultant dynamic equations are given by

$$\tau'_{d0i}\dot{E}'_{qi} = E_{FDi} - E'_{qi} + (x_{di} - x'_{di})I_{di} \tag{3.2}$$

$$\tau'_{q0i}\dot{E}'_{di} = -E'_{di} + (x_{qi} - x'_{qi})I_{qi} \tag{3.3}$$

$$M_i\dot{\omega}_i = P_{mi} - (I_{di}E'_{di} + I_{qi}E'_{qi}) - D_i(\omega_i - \omega_S) \tag{3.4}$$

$$\dot{\delta}_i = \omega_i - \omega_S \qquad i = 1, 2, ..., m \tag{3.5}$$

where,

E'_d, E'_q: direct and quadrature axes stator EMFs corresponding to rotor transient flux components, respectively

I_d, I_q: the d and q axes stator currents

τ'_{d0}, τ'_{q0}: open-circuit direct and quadrature axes transient time constants

x_d, x'_d: direct axis synchronous and transient reactances

x_q, x'_q: quadrature axis synchronous and transient reactances

E_{FD}: stator EMF corresponding to the field voltage

D: damping coefficient

3.2 Excitation System Modeling

The block diagram of the exciter model [24] is shown in Figure 3.1 and all components in this model are static or stationary. The variables are E_{FD}, X_{E1}, and X_{E2}. The dynamic equations for the variables are given by

$$\dot{E}_{FDi} = \frac{K_{Ai}}{T_{Ai}X_{E2i}} - \frac{1}{T_{Ai}}E_{FDi} \tag{3.6}$$

$$\dot{X}_{E1i} = -\frac{1}{T_{Ri}}X_{E1i} + \frac{1}{T_{Ri}}V_{Ti} \tag{3.7}$$

$$\dot{X}_{E2i} = \frac{1}{T_{Bi}}(\frac{T_{Ci}}{T_{Ri}} - 1)X_{E1i} - \frac{1}{T_{Bi}}X_{E2i}$$

$$\qquad -\frac{T_{Ci}}{T_{Bi}T_{Ri}}V_{Ti} + \frac{1}{T_{Bi}}(V_{REFi} + V_{Si}) + \frac{T_{Ci}}{T_{Bi}}\dot{V}_{Si} \tag{3.8}$$

$$V_T = V_{Tq} + jV_{Td}$$

$$\quad = (E'_q + x'_d I_d) + j(E'_d - x'_q I_q) \qquad i = 1, 2, ..., m \tag{3.9}$$

where,

V_T: generator terminal voltage

V_{REF}: exciter reference voltage

$\omega_{\Delta i}(= \frac{\omega_i - \omega_S}{\omega_S})$: power system stabilizer input (speed deviation in p.u.)

3.3 Network Modeling

The network is represented classically: quasi state-steady network parameters, constant impedance loads, etc. Assuming the generator internal reactance to be constant, a network representation at the internal generator nodes can be obtained. A network Y_{bus} consists of $Y_{ij}\angle\theta_{ij} = G_{ij} + jB_{ij}$. The procedure described in chapter 9 of [23] yields the direct and quadrature axes currents for the generators represented in detail. The currents for the classically represented machines can also be obtained. In this case, for
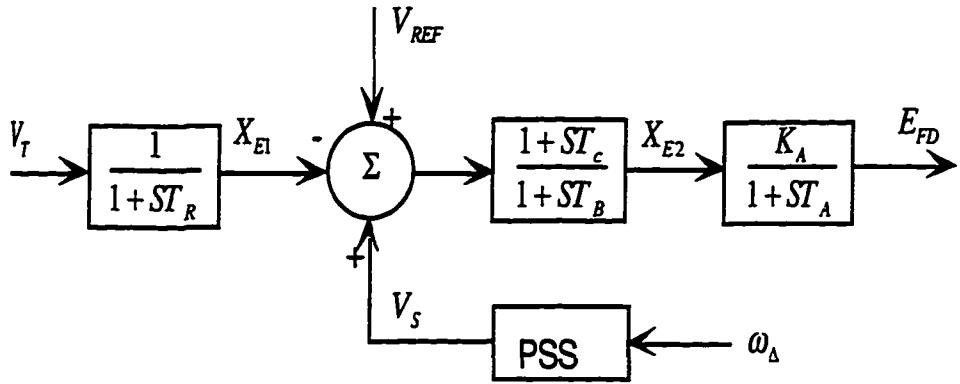
Figure 3.1   Static exciter model

the classical generators $E'_d = 0$ and $E'_q = E = constant$. Then the generator currents are given by

$$I_{qi} = \sum_{j=1}^{m}[F_{G+B}(\delta_{ij})E'_{qj} - F_{B-G}(\delta_{ij})E'_{dj}] + \sum_{k=m+1}^{n} F_{G+B}(\delta_{ik})E_k \qquad (3.10)$$

$$I_{di} = \sum_{j=1}^{m}[F_{B-G}(\delta_{ij})E'_{qj} + F_{G+B}(\delta_{ij})E'_{dj}] + \sum_{k=m+1}^{n} F_{B-G}(\delta_{ik})E_k \qquad (3.11)$$

$$I_k = \sum_{j=1}^{m}[F_{G+B}(\delta_{ij})E'_{qj} - F_{B-G}(\delta_{ij})E'_{dj}] + \sum_{l=m+1}^{n} F_{G+B}(\delta_{kl})E_l \qquad (3.12)$$

$$i = 1, 2, ..., m \qquad\qquad k, l = m + 1, ..., n$$

where

$$F_{G+B}(\delta_{ij}) \;=\; G_{ij}cos(\delta_{ij}) + B_{ij}sin(\delta_{ij}) \qquad (3.13)$$

$$F_{G-B}(\delta_{ij}) \;=\; B_{ij}cos(\delta_{ij}) - G_{ij}sin(\delta_{ij}) \qquad (3.14)$$

$$\delta_{ij} \;=\; \delta_i - \delta_j \qquad (3.15)$$

3.4 System Equation

The dynamic equations governing the generators and the excitation system have the general form

$$\dot{x} = f(x) \tag{3.16}$$

where,

$$x = [E'_{q1}, E'_{d1}, \omega_1, \delta_1, E_{FD1}, x_{E1_1}, x_{E2_1}, \ldots, E'_{qm}, E'_{dm}, \omega_m, \delta_m, E_{FDm}, x_{E1_m}, x_{E2_m}, \ldots, \omega_n, \delta_n]^T,$$

and f is an analytic vector field which maps $\mathbf{R}^N$ into $\mathbf{R}^N$ and is continuously differentiable. The vector f is made up of seven functions as given below.

$$
\begin{aligned}
f_{1i} &= \dot{E}'_{qi} \\
&= \frac{1}{\tau'_{d0i}}[E_{FDi} - E'_{qi} + (x_{di} - x'_{di})I_{di}] && i = 1, \ldots, m && (3.17) \\
f_{2i} &= \dot{E}'_{di} \\
&= \frac{1}{\tau'_{q0i}}[-E'_{di} + (x_{qi} - x'_{qi})I_{qi}] && i = 1, \ldots, m && (3.18) \\
f_{3i} &= \dot{\omega}_i \\
&= \frac{1}{M_i}[P_{mi} - (I_{di}E'_{di} + I_{qi}E'_{qi}) - D_i(\omega_i - \omega_S) && i = 1, \ldots, n && (3.19) \\
f_{4i} &= \dot{\delta}_i \\
&= \omega_i - \omega_S && i = 1, \ldots, n && (3.20) \\
f_{5i} &= \dot{E}_{FDi} \\
&= \frac{K_{Ai}}{T_{Ai}X_{E2i}} - \frac{1}{T_{Ai}}E_{FDi} && i = 1, \ldots, m && (3.21) \\
f_{6i} &= \dot{X}_{E1i} \\
&= -\frac{1}{T_{Ri}}X_{E1i} + \frac{1}{T_{Ri}}V_{Ti} && i = 1, \ldots, m && (3.22) \\
f_{7i} &= \dot{X}_{E2i}
\end{aligned}
$$

$$= \frac{1}{T_{Bi}}(\frac{T_{Ci}}{T_{Ri}} - 1)X_{E1i} - \frac{1}{T_{Bi}}X_{E2i}$$

$$-\frac{T_{Ci}}{T_{Bi}T_{Ri}}V_{Ti} + \frac{1}{T_{Bi}}(V_{REFi} + V_{Si}) + \frac{T_{Ci}}{T_{Bi}}\dot{V}_{Si} \qquad i = 1, ..., m \qquad (3.23)$$

A point, $\mathbf{x}_{ep}$ is called as an equilibrium point if $\mathbf{f}(\mathbf{x}_{ep}) = 0$. We assume that the total order of the system (3.16) is N. The system of N equations represent $(N - 1)$ independent equations and can be reduced from N to $N - 1$ by introducing the relative angles.

4 EIGENANALYSIS AND NORMAL FORMS OF VECTOR FIELDS

4.1 Eigenanalysis

Linear systems can be described by either the input-output description, or the state-variable description. Once these descriptions are obtained, we can analyze them qualitatively and quantitatively. In the qualitative analyses, we are interested in the general properties, such as controllability, observability, participation factors and stability, of the equations. In the quantitative analyses, we are interested in the exact responses of equations due to some excitation. Digital computers can be used to carry out these analyses. However computer solutions are not in closed forms, and it is difficult to extrapolate any properties from these solutions.

Because of the powerful tools we know for linear systems, the first step in analyzing a nonlinear system (3.16) is to linearize it about some nominal operating point and analyze the resulting linear model. If the operating range of a system is small, and if the involved nonlinearities are smooth, then the system may be reasonably approximated by a linearized system having dynamics described by a set of linear differential equations. In order to find the general properties of the dynamical equation (3.16), we apply the qualitative analyses on the linearized equation (4.2) of (3.16) (see chapter 1 of [25]). An important concept in dealing with the linearized equation is the concept of an equilibrium point. A point $x = x_{ep}$ in the state-space is said to be an equilibrium point of (3.16) if it has the property that whenever the state of the system starts at x_{ep} it will remain at

x_{ep} for all future time. For the equation (3.16), the equilibrium points are the real roots of the equation (4.1).

$$f(x) = 0 \qquad (4.1)$$

The dynamics of the linearized system of (3.16) at x_{ep} are of the form

$$\dot{x} = Ax \qquad (4.2)$$

where,

$$A = [\partial f / \partial x]_{x_{ep}}$$

In order to determine the stability of x_{ep}, we must understand the nature of solutions near x_{ep}. Let

$$x = x_{ep} + x_r \qquad (4.3)$$

Substituting (4.3) into (3.16) and obtaining the Taylor's series about x_{ep} gives

$$\dot{x} = \dot{x}_{ep} + \dot{x}_r = f(x_{ep}) + Ax_r + H.O.T. \qquad (4.4)$$

Using the fact that $\dot{x}_{ep} = f(x_{ep})$, (4.4) becomes

$$\dot{x}_r = Ax_r + H.O.T. \qquad (4.5)$$

Equation (4.5) describes the evolution of orbits near x_{ep}. For stability questions we are concerned with the behavior of solutions arbitrarily close to x_{ep}, so it seems reasonable that this question could be answered by studying the associated linear system

$$\dot{x}_r = Ax_r \qquad (4.6)$$

Therefore the solution of (4.6) through the point $x_r(0)$ of $t = 0$ can be written as

$$x_r(t) = e^{At}x_r(0) \tag{4.7}$$

Thus, $x_r(t)$ (i.e. $x_{ep}(t)$) is asymptotically stable if all eigenvalues of A have negative real parts.

Eigenvalues are defined as the solutions to the matrix equation

$$det[\lambda I - A] = 0 \tag{4.8}$$

where the parameters λ are called the eigenvalues.

A vector u is called an eigenvector of A if u satisfies the equation (4.9).

$$Au = \lambda u \tag{4.9}$$

Similarly a vector v is called an left eigenvector of A if v satisfies equation (4.10).

$$A^T v = \lambda v \tag{4.10}$$

Whereas each eigenvector has a unique eigenvalue associated with it, each eigenvalue is associated with many eigenvectors. The following propositions concern important properties of the eigenvalues and eigenvectors of an $N \times N$ matrix A:

1. The eigenvalues of A (not necessarily distinct)

$$\lambda(A) = \lambda_1, ..., \lambda_N$$

are the N roots of the characteristic equation (which is a polynomial of the N-th degree in λ).

2. A linear combination of eigenvectors associated with the same eigenvalue is also an eigenvector associated with that same eigenvalue. In particular if x is an eigenvector, then cx, where $c \neq 0$ is constant, is also an eigenvector.

3. Any left (right) eigenvector of $\mathbf{A}$ is orthogonal to any right (left) eigenvector of $\mathbf{A}$ except its own pair:

$$\mathbf{v}_i^T \mathbf{u}_j \begin{cases} = 0 & \text{for } i \neq j \\ \neq 0 & \text{for } i = j \end{cases} \qquad (i, j = 1, ..., N)$$

where the eigenvectors have been normalized so that $\mathbf{v}_i^T \mathbf{u}_i = 1 (i = 1, ..., N)$.

4. Let the $N \times N$ matrix $\mathbf{A}$ have N linearly independent right eigenvectors $\mathbf{u}_1, ..., \mathbf{u}_N$. Therefore the set of vectors $\mathbf{u}_1, ..., \mathbf{u}_N$ can serve as a basis for the N-dimensional vector space $\mathbf{R}^N$. Any N-component vector $\mathbf{x}$ can be expressed in the new basis as

$$\mathbf{x} = \sum_{i=1}^{N} x_{Ti} \mathbf{u}_i = \mathbf{U} \mathbf{x}_T$$

where x_{Ti} is the i-th component of the transformed vector $\mathbf{x}_T$ and

$$\mathbf{U} = [\mathbf{u}_1 \ ... \ \mathbf{u}_N]$$

is the right modal matrix of $\mathbf{A}$. The left modal matrix $\mathbf{V}$ can be defined in the same fashion

$$\mathbf{V}^T = \begin{bmatrix} \mathbf{v}_1^T \\ ... \\ \mathbf{v}_N^T \end{bmatrix}$$

and, assuming that the left eigenvectors have been normalized as indicated before

$$\mathbf{V}^T = \mathbf{U}^{-1}$$

so that the variable transformation can also be written as

$$\mathbf{x}_T = \mathbf{V}^T \mathbf{x}$$

4.1.1 An Example of Eigenanalysis

The following example is borrowed from [26].

Assume that the population of a country is divided into three distinct segments, rural, urban and suburban. The natural growth rates with respect to time due to procreation in the three segments are equal to α_r, α_u and α_s, respectively. The population distribution, however, is modified by migration between the different segments. The rate of this migration is in part influenced by the need for a base of rural activity that is adequate to support the total population of the country, the optimal rural base being a given fraction γ of the total population. The rate of migration from the rural to the urban area is proportional to the excess of rural population over the optimal rural base, with β being the proportionality factor. If the rural, urban and suburban populations at a certain time t are denoted by $x_r(t)$, $x_u(t)$ and $x_s(t)$, respectively, then the total population is $x_r(t)+x_u(t)+x_s(t)$, the optimal rural base is $\gamma[x_r(t)+x_u(t)+x_s(t)]$, and thus the excess rural population is $x_t(t) - \gamma[x_r(t)+x_u(t)+x_s(t)]$. Another migration pattern takes place between the urban and suburban segments, with the net effect being that the urban population moves to the suburbs at a rate that is proportional to the amount of urban population itself. The proportionality factor is denoted by δ. A simple continuous-time model of the migration process, based on the above assumptions, is then

$$\frac{dx_s(t)}{dt} = \alpha_s x_s(t) + \delta x_u(t)$$

$$\frac{dx_u(t)}{dt} = \alpha_u x_u(t) + \beta x_r(t) - \gamma[x_r(t) + x_u(t) + x_s(t)] - \delta x_u(t)$$

$$\frac{dx_r(t)}{dt} = \alpha_r x_r(t) - \beta x_r(t) - \gamma[x_r(t) + x_u(t) + x_s(t)]$$

or, in state vector form (4.2),

$$\dot{\mathbf{x}} = \mathbf{A}\mathbf{x}$$

where

$$\mathbf{x} = \begin{bmatrix} x_s \\ x_u \\ x_r \end{bmatrix}$$

and

$$\mathbf{A} = \begin{bmatrix} \alpha_s & \delta & 0 \\ -\beta\gamma & \alpha_u - \beta\gamma - \delta & \beta(1-\gamma) \\ \beta\gamma & \beta\gamma & \alpha_r - \beta(1-\gamma) \end{bmatrix}$$

Assume that:

$$\alpha_s = 0.045(10 years)^{-1}$$

$$\alpha_r = 0.050(10 years)^{-1}$$

$$\alpha_u = 0.055(10 years)^{-1}$$

$$\delta = 0.200(10 years)^{-1}$$

$$\beta = 0.100(10 years)^{-1}$$

$$\gamma = 0.200$$

Each of these parameters might normally change with time, but they are assumed to be constant for purposes of this example. The resulting $\mathbf{A}$ matrix is:

$$A = \begin{bmatrix} 0.045 & 0.200 & 0.0 \\ -0.020 & -0.165 & 0.080 \\ 0.020 & 0.020 & -0.030 \end{bmatrix}$$

Our first objective will be to understand the various patterns of behavior built into the model. Examination of the eigenvalues and eigenvectors of the system matrix A is the commonly used approach. The results of eigenanalysis of A are:

Eigenvalues:

$$\begin{bmatrix} \lambda_1 & 0 & 0 \\ 0 & \lambda_2 & 0 \\ 0 & 0 & \lambda_3 \end{bmatrix} = \begin{bmatrix} 0.046 & 0 & 0 \\ 0 & -0.143 & 0 \\ 0 & 0 & -0.053 \end{bmatrix}$$

Right eigenvectors:

$$U = \begin{bmatrix} u_1 & u_2 & u_3 \end{bmatrix} = \begin{bmatrix} 1.0 & 1.0 & 1.0 \\ 0.005 & -0.939 & -0.492 \\ 0.264 & -0.011 & -0.438 \end{bmatrix}$$

Left eigenvectors:

$$V^T = \begin{bmatrix} v_1^T \\ v_2^T \\ v_3^T \end{bmatrix} = \begin{bmatrix} 0.770 & 0.811 & 0.852 \\ -0.243 & -1.335 & 0.947 \\ 0.473 & 0.524 & -1.799 \end{bmatrix}$$

which have been normalized so that

$$UV^T = V^TU = I \tag{4.11}$$

Several things can be learned from the above results. The only growing natural mode ($\lambda_1 = 0.046$) must reflect the overall population growth. This is the dominant mode and the entries in the associated right eigenvector define the relative distribution of population ($x_s = 1.0, x_u = 0.005, x_r = 0.264$) that will be reached in the long run, when all the other dynamics have vanished. This is also the initial relative distribution of population that is needed in order for all variables to have a purely exponential growth with $\lambda_1 = 0.046$. However, given any initial population distribution x(0), in general the three natural modes will be excited, with the left eigenvectors determining the share of the initial state x(0) corresponding to each mode

$$x(0) = [v_1^T x(0)]u_1 + [v_2^T x(0)]u_2 + [v_3^T x(0)]u_3 \qquad (4.12)$$

and thus with the following natural time response

$$x(t) = \sum_{i=1}^{3}[v_i^T x(0)]u_i e^{\lambda_i t} \qquad (4.13)$$

The exponentially decreasing modes 2 and 3 describe how any deviation in the population distribution with respect to the proportions given by u_1 will evolve with time, eventually vanishing. The second natural mode ($\lambda_2 = -0.143$) basically concerns surpluses (deficiencies) in the urban population combined with deficiencies (surpluses) in the suburban one, which excite the dynamic pattern of migration between the urban and suburban areas. This can be seen from the value of λ_2 itself, which is close to $\alpha_u - \delta$, and also from the entries of the right eigenvector u_2 showing that large and almost opposite values of x_u and x_s (that only require a very small base of rural population) are all that is needed to excite this mode. Similarly, the third natural mode ($\lambda_3 = -0.053$) concerns surpluses (deficiencies) in both the urban and rural population combined with deficiencies (surpluses) in the suburban one. Thereby the two existing migration patterns are significantly active in this mode. In all three modes the corresponding left eigenvector

also tells us what linear combination $v_i^T x(0)$ of the original states is the precise system variable that varies exponentially as λ_i. Therefore the entries of v_i^T also provide an indication of the level of involvement of the various state variables in the i-th natural mode. This issue will be discussed later in more detail. It must be realized that slightly different numerical values of the system parameters may yield substantially different dynamic behaviors. For instance, with $\alpha_s = 0.04$, $\alpha_r = 0.05$, $\alpha_u = 0.06$, $\delta = 0.10$, $\beta = 0.07$ and $\gamma = 0.20$, the eigenvalues are 0.043 and $-0.031 \pm j0.015$, indicating that there is an oscillatory pattern superimposed to the overall exponential population growth.

There is seemingly no difficulty with the proposed task. Complete eigenanalysis of the entire model can be performed for each scenario. Then, inspection of the eigenvalues and eigenvectors will provide the desired understanding of the model, as was shown before.

4.2 The Normal Forms of Vector Fields

4.2.1 Normal Form Theorem and Transformation

From chapter 2 of [25]: The method of normal forms provides a way of finding a coordinate system in which the dynamical system takes the simplest form. As we develop the method, three important characteristics should become apparent.

1. *"The method is local in the sense that the coordinate transformations are generated in a neighborhood of a known solution. For our purposes, the known solution will be an equilibrium point."*

2. *"In general, the coordinate transformations will be nonlinear functions of the dependent variables. These coordinate transformations are found by solving a sequence of linear problems."*

3. *"The structure of the normal form is determined entirely by the nature of the linear part of the vector field."*

Consider the vector field (3.16). First we expand (3.16) as a Taylor's series about a stable equilibrium point x_{SEP} which is the equilibrium point where the linearized system is stable, and obtain using again x and x_i as the state variables.

$$\dot{x}_i = A_i x + \frac{1}{2} x^T H^i x + H.O.T. \quad (i = 1, 2, ..., N) \tag{4.14}$$

where,

$$A_i = i_{th} \text{ row of Jacobian A which is equal to } [\partial f/\partial x]_{x_{SEP}}$$

$$H_i = [\partial^2 f_i/\partial x_j \partial x_k]_{x_{SEP}} = \text{Hessian matrix}$$

Denote by J the (complex) Jordan form of A, and by U the matrix of the right eigenvectors of A. Then the transformation $x = Uy$ yields for the linear and the 2nd order terms of (4.15) the equivalent system

$$\dot{y}_j = \lambda_j y_j + \sum_{k=1}^{N} \sum_{l=1}^{N} C_{kl}^j y_k y_l + H.O.T. \quad (j = 1, 2, ..., N) \tag{4.15}$$

where,

$$C^j = \frac{1}{2} \sum_{p=1}^{N} V_{jp}^T [U^T H^p U] = [C_{kl}^j] \quad (j, k, l = 1, 2, ..., N)$$

and V denotes the matrix of associated left eigenvectors. If the 2nd order non-resonance condition holds, i.e. if $\lambda_j \neq \lambda_k + \lambda_l$ for all three tuples of eigenvalues of A, then the normal form transformation of (4.15) is defined by

$$y = z + h2(z) \tag{4.16}$$

where,

$$h2^j(z) = \sum_{k=1}^{N} \sum_{l=1}^{N} h2_{kl}^j z_k z_l \quad (j = 1, 2, ..., N)$$

$$h2_{kl}^j = \frac{C_{kl}^j}{\lambda_k + \lambda_l - \lambda_j} \qquad (j, k, l = 1, 2, ..., N)$$

The chosen **h2(z)** is of a specific form to simplify the high order terms as much as possible.

In the z-coordinates, the system (4.15) takes on the form

$$\dot{z}_j = \lambda_j z_j + H.O.T. \qquad (j = 1, 2, ..., N) \tag{4.17}$$

Equations (4.14)-(4.17) allow us to obtain explicit 2nd order solutions for the system in the different coordinate systems. In the z-coordinates the solution of (4.17) is given by

$$z_j(t) = z_{jo} e^{\lambda_j t} \qquad (j = 1, 2, ..., N) \tag{4.18}$$

where z_{jo} represents the initial condition.

According to (4.16), the closed solution in the y-coordinates can be expressed by

$$y_j(t) = z_j(t) + h2^j(z(t)) \qquad (j = 1, 2, ..., N) \tag{4.19}$$

Substituting for $z_j(t)$ from (4.18), we have

$$y_j(t) = z_{jo} e^{\lambda_j t} + \sum_{k=1}^{N} \sum_{l=1}^{N} h2_{kl}^j z_{ko} z_{lo} e^{(\lambda_k + \lambda_l)t} \qquad (j = 1, 2, ..., N) \tag{4.20}$$

The transformation **x = Uy** gives the solution in x-coordinates as

$$x_i(t) = \sum_{j=1}^{N} U_{ij} z_{jo} e^{\lambda_j t} + \sum_{j=1}^{N} U_{ij} [\sum_{k=1}^{N} \sum_{l=1}^{N} h2_{kl}^j z_{ko} z_{lo} e^{(\lambda_k + \lambda_l)t}] \qquad (i = 1, 2, ..., N) \tag{4.21}$$

In the above analysis the initial condition z_o plays an important role. The details of obtaining z_o are given in Appendix A.

4.2.2 The Quantification of 2nd order Nonlinear Modal Interaction

The presence of the nonlinear modal interaction has strong effect on system performance. Therefore the quantification of nonlinear modal interaction is needed to understand and control the interactions. For this purpose we introduce several indices.

4.2.2.1 Nonlinear Interaction Index (I1) [27]

Let us start from the Jordan variable space $y \in \mathbf{C}^d$, where d is the appropriate dimension for the generator and/or control variables. The h2 transformation maps the z-space into the y-space via (4.22)

$$y_j(t) = z_j(t) + h2^j(z(t)) \qquad (j = 1, 2, ..., d) \tag{4.22}$$

Assuming no 2nd order resonance, i.e. $\lambda_k + \lambda_l - \lambda_j \neq 0$ for all k, l, and j, the system in z-space is linear.

$$\dot{\mathbf{z}} = \mathbf{J}\mathbf{z} \tag{4.23}$$

where, $\mathbf{J}$ is the Jordan form of the linear term of the system equations, i.e. $\mathbf{J}$ is a complex, diagonal $d \times d$ matrix. Equation (4.23) is solved as

$$z_j(t) = z_{jo}e^{\lambda_j t} \qquad (j = 1, 2, ..., d) \tag{4.24}$$

where z_{jo} is the initial value.

The corresponding solution of (4.22) is

$$y_j(t) = z_{jo}e^{\lambda_j t} + \sum_{k=1}^{d} \sum_{l=k}^{d} h2_{kl}^j z_{ko} z_{lo} e^{(\lambda_k + \lambda_l)t} \qquad (j = 1, 2, ..., d) \tag{4.25}$$

which contains all 2nd order terms corresponding to the normal form (4.22) and (4.23). Note that the r.h.s. of (4.25) contains influences of the nonlinearity in both terms: In z_{jo}

the nonlinear coordinate transformation (4.22) is reflected only in the initial value, in the second term the 2nd order correction of the solution due to nonlinear modal interaction is represented. The linear system in y-space is

$$\dot{\mathbf{y}} = \mathbf{J}\mathbf{y} \qquad (4.26)$$

with solution

$$\bar{y}_j(t) = y_{jo}e^{\lambda_j t} \qquad (j = 1, 2, ..., d) \qquad (4.27)$$

which corresponds to the linearization of the original system alone. The comparison of (4.24), (4.25), and (4.27) yield various indices, which will be discussed below. Note first of all that $h2_{kl}^j$ is large, and it contributes to the second term in (4.25), if

a) C_{kl}^j is large

b) $\lambda_k + \lambda_l - \lambda_j$ is small, i.e. $\lambda_j \approx \lambda_k + \lambda_l$

Comparing (4.24) and (4.27), we can assess the influence of the nonlinear effect on the initial value by considering

$$|\bar{y}_j(t) - z_j(t)| = |y_{jo} - z_{jo}|e^{\lambda_j t} \qquad (j = 1, 2, ..., d) \qquad (4.28)$$

or simply

(A) $|y_{jo} - z_{jo}|$

because the entire solutions just scale this initial distance with $e^{\lambda_j t}$. Hence if (A) is large, the distance between (4.24) and (4.27) the nonlinear influence on the initial value is large. To this term which represents the difference in the linear part of the approximate

solution and the linear solution, we add the 2nd order terms to capture the effect of the nonlinearities on the difference between the terms. Hence we obtain

$$|(y_{jo} - z_{jo})e^{\lambda_j t} + \sum_{k=1}^{d} \sum_{l=k}^{d} h2_{kl}^{j} z_{ko} z_{lo} e^{(\lambda_k + \lambda_l)t}| \qquad (j = 1, 2, ..., d) \qquad (4.29)$$

The expression (4.29) is unwieldy for fast computations in large systems, so we make two approximations

a) We consider only the largest term $h2_{kl}^{j} z_{ko} z_{lo}$ and assume that all other terms are small compared to the largest one.

b) We note, as above, that $h2_{kl}^{j}$ is large if $\lambda_j \approx \lambda_k + \lambda_l$.

and the corresponding index is

$$I1(j) = |(y_{jo} - z_{jo}) + \max_{k,l} h2_{kl}^{j} z_{ko} z_{lo}| \qquad (j = 1, 2, ..., d) \qquad (4.30)$$

where $\max_{k,l} h2_{kl}^{j} z_{ko} z_{lo}$ is the complex form when $\max_{k,l} |h2_{kl}^{j} z_{ko} z_{lo}|$ occurs.

This is called "nonlinear interaction index" and identifies the dominant modal interaction.

4.2.2.2 Nonlinearity Index (I2)

Similarly, the relative amount of the 2nd order nonlinearity at mode j can be expressed by the relative size of (4.24) and (4.25).

$$|\frac{y_j(t)}{z_j(t)}| = |\frac{z_{jo}e^{\lambda_j t} + \sum_{k=1}^{d} \sum_{l=k}^{d} h2_{kl}^{j} z_{ko} z_{lo} e^{(\lambda_k + \lambda_l)t}}{z_{jo}e^{\lambda_j t}}| \qquad (j = 1, 2, ..., d) \qquad (4.31)$$

If we consider same approximations as before, then it leads to

$$|\frac{y_j(t)}{z_j(t)}| \approx |1 + \frac{max_{k,l} h2_{kl}^{j} z_{ko} z_{lo}}{z_{jo}}| \leq 1 + |\frac{max_{k,l} h2_{kl}^{j} z_{ko} z_{lo}}{z_{jo}}| \qquad (j = 1, 2, ..., d) \qquad (4.32)$$

From this equation we introduce the "nonlinearity index" I2 which is defined as

$$I2(j) = \frac{\max_{k,l} h2_{kl}^j z_{ko} z_{lo}}{z_{jo}} \qquad (j = 1, 2, ..., d) \qquad (4.33)$$

The nonlinearity index is a measure of the relative size of the nonlinearity in the initial value and represents the normalized severity of nonlinear interaction.

4.2.2.3 Second order interaction coefficients

The 2nd order interaction coefficients of mode j are defined as

$$h2_{kl}^j z_{ko} z_{lo} \qquad (k, l = 1, 2, ..., d) \qquad (4.34)$$

as they appear in equations (4.20) and (4.21). Since the nonlinear part of explicit 2nd order solutions for the system depends on the $h2_{kl}^j z_{ko} z_{lo}$, this can represent the effect of the higher order terms of mode j with mode k and mode l.

4.2.3 Participation Factors

4.2.3.1 Linear Participation Factors

Linear participation factors are a well-known method of identifying mode-machine interactions [28], and for their definition an interpretation of the meaning of the right and left eigenvectors needs to be given now. A right eigenvector u_i can be seen as a particular value of the state x. If the state $x(0)$ points initially in the direction of a right eigenvector u_i it will continue to point in the same direction although its magnitude may change, and therefore only the corresponding i-th natural mode excited. In the case of independent eigenvectors, the initial state $x(0)$ can always be expressed as a linear combination of the N right eigenvectors, with the weighting coefficients each changing with time. On the other hand a left eigenvector v_i is more naturally interpreted as

defining the scalar function of the state variables

$$x_{Ti} = \mathbf{v}_i^T \mathbf{x}$$

which is exclusively associated to the i-th natural mode. A left eigenvector $\mathbf{v}_i$ defines a certain linear combination of the components $\mathbf{x}_k$ of the state vector. The entries of $\mathbf{v}_i$ are the proper weights of the states $\mathbf{x}_k$ that yield the decoupled variable x_{Ti}. Therefore, the participation factor p_{ki} represents a measure of the participation of the k-th machine state in the trajectory of the i-th mode. It is given by

$$p_{ki} = U_{ki} * V_{ki} \qquad (4.35)$$

Since linear participation factors are functions of both the left and right eigenvectors, they are independent of eigenvector scaling. They have been used to determine the site of the control, and to classify modes of the system into different groups such as interarea modes, control modes, and local plant modes; we will make useof them in this latter way.

4.2.3.2 Nonlinear Participation Factors

For analyzing the modal interactions we need to use a new concept of participation factors, the nonlinear participation factors which could identify the participating states in the combinational modes. Using normal forms, we apply the nonlinear participation factor [29]. The normal form initial conditions, using the 2nd order approximation of the inverse transformation (4.16), can be used to express the solution for k-th machine state variable as

$$x_k(t) = \sum_{i=1}^{N} U_{ki}(V_{ik} + v_{2ikk})e^{\lambda_i t} + \sum_{p=1}^{N}\sum_{q=p}^{N} u_{2kpq}(V_{pk} + v_{2pkk})(V_{qk} + v_{2qkk})e^{(\lambda_p + \lambda_q)t} \qquad (4.36)$$

$$(k = 1, 2, ..., N)$$

where $u2_{ikl}$ and $v2_{ipp}$ are the elements of 2nd order right eigenvector and 2nd order left eigenvector, and these are given by

$$v2_{ipp} = -\sum_{k=1}^{N}\sum_{l=1}^{N} h2_{kl}^{i}V_{kp}V_{lp}$$

$$u2_{ikl} = \sum_{j=1}^{N} U_{ij}h2_{kl}^{j}$$

Using the approach given in [29], one can define 2nd order participation factors according to

$$x_k(t) = \sum_{i=1}^{N} p2_{ki}e^{\lambda_i t} + \sum_{p=1}^{N}\sum_{q=p}^{N} p2_{kpq}e^{(\lambda_p+\lambda_q)t} \quad (k=1,2,...,N) \qquad (4.37)$$

where,

$$p2_{ki} = U_{ki}(V_{ik} + v_{2ikk})$$

$$p2_{kpq} = u2_{kpq}(V_{pk} + v2_{pkk})(V_{qk} + v2_{qkk})$$

Note that there are two types of 2nd order participation factors. The $p2_{ki}$ represents the 2nd order participation of the k-th machine state in the i-th single eigenvalue mode. In fact, the linear participation factor, p_{ki}, is one term in the expression for $p2_{ki}$ which includes the 2nd order corrections. The $p2_{kpq}$ represents the 2nd order participation of the k-th machine state in the 'mode' formed by the combination of the p and q modes. This can be used to provide the participating states at the combination modes which have strong interactions with the critical modes.

5 SENSITIVITY ANALYSIS

5.1 Eigenvalue Sensitivity

Based on the eigenanalysis in the previous chapter, the free motions of a dynamical system governed by the equation:

$$\dot{x} = Ax \tag{5.1}$$

are given by the expression:

$$x(t) = \sum_{i=1}^{N} u_i v_i^T x(0) e^{\lambda_i t} \tag{5.2}$$

In equation (5.1), x is the $N \times 1$ state vector of the system, A is an $N \times N$ matrix with distinct eigenvalues $\lambda_i (i = 1, 2, ..., N)$: in (5.2), $u_i (i = 1, 2, ..., N)$ are the linearly independent eigenvectors of A which satisfy:

$$Au_i = \lambda_i u_i \tag{5.3}$$

and $v_j (j = 1, 2, ..., N)$ are the corresponding eigenvectors of A^T which satisfy:

$$v_j^T A = \lambda_j v_j^T \tag{5.4}$$

u_i and v_j satisfy the equation:

$$\mathbf{u}_i^T \mathbf{v}_j = \mathbf{v}_j^T \mathbf{u}_i \begin{cases} = 0 & \text{for } i \neq j \\ \\ \neq 0 & \text{for } i = j \end{cases} \qquad (i, j = 1, ..., N) \qquad (5.5)$$

The corresponding fundamental problem in sensitivity theory is to determine the sensitivities of λ_i, $\mathbf{u}_i$, $\mathbf{v}_i (i = 1, 2, ..., N)$ to changes in system parameters, i.e. to changes in the elements of the matrix $\mathbf{A}$ [30, 31]. In power system (3.16) the vector field f depends on the parameter σ of the exciters present in the system, as do all the terms of the Taylor's series (4.14) including $\mathbf{A}$. If $\mathbf{A} = [a_{kl}]$ and the element a_{kl} is perturbed due to changes in system parameter σ, then the eigenvalues and eigenvectors of $\mathbf{A}$ will change. Indeed, partial differentiation of equation (5.3) with respect to a_{kl} indicates that

$$\frac{\partial \mathbf{A}}{\partial a_{kl}} \mathbf{u}_i + \mathbf{A} \frac{\partial \mathbf{u}_i}{\partial a_{kl}} = \frac{\partial \lambda_i}{\partial a_{kl}} \mathbf{u}_i + \lambda_i \frac{\partial \mathbf{u}_i}{\partial a_{kl}} \qquad (5.6)$$

Pre-multiplication of equation (5.6) by $\mathbf{v}_i^T$ then gives

$$\mathbf{v}_i^T \frac{\partial \mathbf{A}}{\partial a_{kl}} \mathbf{u}_i + \lambda_i \mathbf{v}_i^T \frac{\partial \mathbf{u}_i}{\partial a_{kl}} = \mathbf{v}_i^T \frac{\partial \lambda_i}{\partial a_{kl}} \mathbf{u}_i + \lambda_i \mathbf{v}_i^T \frac{\partial \mathbf{u}_i}{\partial a_{kl}} \qquad (5.7)$$

Using the fact that

$$\frac{\partial \mathbf{A}}{\partial a_{kl}} = [\alpha_{ij}] = [\delta_{ik} \delta_{jl}] \qquad (5.8)$$

equation (5.7) reduces to the set of scalar equations:

$$\frac{\partial \lambda_i}{\partial a_{kl}} = V_{ki} U_{li} \qquad (i, k, l = 1, 2, ..., N) \qquad (5.9)$$

In equation (5.9), V_{ki} and U_{li} are respectively the k-th element of $\mathbf{v}_i$ and the l-th element of $\mathbf{u}_i$. Therefore the desired eigenvalue sensitivity coefficients which relate changes in the λ_i to changes in the σ are given by

$$\frac{\partial \lambda_i}{\partial \sigma} = \mathbf{v}_i^T (\frac{\partial \mathbf{A}}{\partial \sigma}) \mathbf{u}_i \quad (i = 1, 2, ..., N) \tag{5.10}$$

as the sensitivity of the i-th eigenvalue with respect to σ.

5.2   Eigenvector Sensitivity

The eigenvector changes arising from a perturbation of the element a_{kl} of $\mathbf{A}$ can be determined very simply by differentiating both equations (5.3) and (5.4) partially with respect to a_{kl}, and by writing the resulting equations in the form [30, 31]:

$$(\mathbf{A} - \lambda_i \mathbf{I}) \frac{\partial \mathbf{u}_i}{\partial a_{kl}} = \frac{\partial \lambda_i}{\partial a_{kl}} \mathbf{u}_i - \frac{\partial \mathbf{A}}{\partial a_{kl}} \mathbf{u}_i \tag{5.11}$$

$$\frac{\partial \mathbf{v}_j^T}{\partial a_{kl}} (\mathbf{A} - \lambda_j \mathbf{I}) = \frac{\partial \lambda_j}{\partial a_{kl}} \mathbf{v}_j^T - \mathbf{v}_j^T \frac{\partial \mathbf{A}}{\partial a_{kl}} \tag{5.12}$$

Since λ_i and λ_j are eigenvalues of $\mathbf{A}$, the matrices $(\mathbf{A} - \lambda_i \mathbf{I})$ and $(\mathbf{A} - \lambda_j \mathbf{I})$ are singular so that equations (5.11) and (5.12) cannot be solved immediately for the eigenvector sensitivity coefficients $\partial \mathbf{u}_i / \partial a_{kl}$ and $\partial \mathbf{v}_j^T / \partial a_{kl}$.

Nevertheless, if equation (5.11) and (5.12) is pre-multiplied by $\mathbf{v}_j^T (j \neq i)$ and is post-multiplied by $\mathbf{u}_i (i \neq j)$, it follows that

$$(\lambda_j - \lambda_i) \mathbf{v}_j^T \frac{\partial \mathbf{u}_i}{\partial a_{kl}} = -V_{jk} U_{li} \quad (j \neq i; j = 1, 2, ..., N) \tag{5.13}$$

$$\frac{\partial \mathbf{v}_j^T}{\partial a_{kl}} \mathbf{u}_i (\lambda_i - \lambda_j) = -V_{jk} U_{li} \quad (i \neq j; i = 1, 2, ..., N) \tag{5.14}$$

in view of equations (5.5) and (5.8). Now, if equation (5.13) is pre-multiplied by $\mathbf{u}_j (j \neq i)$ and equation (5.14) is post-multiplied by $\mathbf{v}_i^T$, it becomes that

$$\mathbf{u}_j \mathbf{v}_j^T \frac{\partial \mathbf{u}_i}{\partial a_{kl}} = -(\frac{V_{jk} U_{li}}{\lambda_j - \lambda_i}) \mathbf{u}_j \quad (j \neq i; j = 1, 2, ..., N) \tag{5.15}$$

$$\frac{\partial v_j^T}{\partial a_{kl}} u_i v_i^T = (\frac{V_{jk} U_{li}}{\lambda_j - \lambda_i}) v_i^T \quad (i \neq j; i = 1, 2, ..., N) \tag{5.16}$$

Equations (5.15) and (5.16) can be written more compactly by introducing the matricies

$$\mathbf{G}_{ji} = [g_{ji}^{kl}] = \frac{\mathbf{v}_j \mathbf{u}_i^T}{\lambda_i - \lambda_j} \tag{5.17}$$

$$\mathbf{S}_i = \mathbf{v}_i \mathbf{u}_i^T \tag{5.18}$$

In fact, equations (5.15) and (5.16) then become

$$\mathbf{S}_j^T \frac{\partial \mathbf{u}_i}{\partial a_{kl}} = g_{ji}^{kl} \mathbf{u}_j \quad (j \neq i; j = 1, 2, ..., N) \tag{5.19}$$

$$\frac{\partial \mathbf{v}_j^T}{\partial a_{kl}} \mathbf{S}_i^T = -g_{ji}^{kl} \mathbf{v}_i^T \quad (i \neq j; i = 1, 2, ..., N) \tag{5.20}$$

Since the eigenvectors of $\mathbf{A}$ and $\mathbf{A}^T$ are linearly independent because of the assumption of distinct eigenvalues, the required vectors $\frac{\partial \mathbf{u}_i}{\partial a_{kl}}$ and $\frac{\partial \mathbf{v}_j^T}{\partial a_{kl}}$ may be expanded in terms of the $\mathbf{u}_i$ and $\mathbf{v}_j^T$, respectively. Thus, in the first case, let

$$\frac{\partial \mathbf{u}_i}{\partial a_{kl}} = \sum_{m=1}^{N} \phi_m^{ikl} \mathbf{u}_m \tag{5.21}$$

so that

$$\mathbf{S}_j^T \frac{\partial \mathbf{u}_i}{\partial a_{kl}} = \mathbf{u}_j \mathbf{v}_j^T \sum_{m=1}^{N} \phi_m^{ikl} \mathbf{u}_m = \phi_j^{ikl} \mathbf{u}_j \quad (j \neq i; j = 1, 2, ..., N) \tag{5.22}$$

and in the second case let

$$\frac{\partial \mathbf{v}_j^T}{\partial a_{kl}} = \sum_{m=1}^{N} \psi_m^{jkl} \mathbf{v}_m^T \tag{5.23}$$

so that

$$\frac{\partial \mathbf{v}_j^T}{\partial a_{kl}} \mathbf{S}_i^T = (\sum_{m=1}^{N} \psi_m^{jkl} \mathbf{u}_m) \mathbf{u}_i \mathbf{v}_i^T = \psi_i^{jkl} \mathbf{v}_i^T \quad (i \neq j; j = 1, 2, ..., N) \tag{5.24}$$

It now follows by comparing (5.19) with (5.22) and (5.20) with (5.24) that

$$\phi_j^{ikl} = g_{ji}^{kl} \quad (j \neq i; j = 1, 2, ..., N) \tag{5.25}$$

$$\psi_i^{jkl} = -g_{ji}^{kl} \quad (i \neq j; i = 1, 2, ..., N) \tag{5.26}$$

If the results given in equations (5.25) and (5.26) are now used in equations (5.21) and (5.23), the latter equations become

$$\frac{\partial \mathbf{u}_i}{\partial a_{kl}} = \phi_i^{ikl} \mathbf{u}_i + \sum_{j=1, j \neq i}^{N} g_{ji}^{kl} \mathbf{u}_j \quad (i, k, l = 1, 2, ..., N) \tag{5.27}$$

$$\frac{\partial \mathbf{v}_j^T}{\partial a_{kl}} = \psi_j^{jkl} \mathbf{v}_j^T - \sum_{i=1, i \neq j}^{N} g_{ji}^{kl} \mathbf{v}_i^T \quad (i, k, l = 1, 2, ..., N) \tag{5.28}$$

which give the required eigenvector sensitivity coefficients. The coefficients ϕ_i^{ikl} and ψ_j^{jkl} may be left as completely arbitrary coefficients unless it is desired to constrain the perturbed eigenvectors to satisfy conditions of the form (5.5). If this is the case, then the coefficients must be such that

$$(\mathbf{v}_j^T + d\mathbf{v}_j^T)(\mathbf{u}_i + d\mathbf{u}_i) = (\mathbf{v}_j^T + \frac{\partial \mathbf{v}_j^T}{\partial a_{kl}} da_{kl})(\mathbf{u}_i + \frac{\partial \mathbf{u}_i}{\partial a_{kl}} da_{kl}) = \delta_{ij} \tag{5.29}$$

It can be readily verified by substituting from equations (5.27) and (5.28) into (5.29) that the latter equations will be satisfied to first order of approximation if

$$\phi_i^{ikl} = -\psi_i^{ikl} = \zeta_i^{kl} \quad (i = 1, 2, ..., N)$$

Equations (5.27) and (5.28) for the eigenvector sensitivity coefficients will then have the form

$$\frac{\partial \mathbf{u}_i}{\partial a_{kl}} = \zeta_i^{kl} \mathbf{u}_i + \sum_{j=1,j\neq i}^{N} g_{ji}^{kl} \mathbf{u}_j \quad (i,k,l = 1,2,...,N) \tag{5.30}$$

$$\frac{\partial \mathbf{v}_j^T}{\partial a_{kl}} = -\zeta_j^{kl} \mathbf{v}_j^T - \sum_{i=1,i\neq j}^{N} g_{ji}^{kl} \mathbf{v}_i^T \quad (j,k,l = 1,2,...,N) \tag{5.31}$$

where the ζ_i^{kl} are arbitrary. However, the most convenient choice is perhaps

$$\zeta_i^{kl} = 0 \quad (i,k,l = 1,2,...,N)$$

Therefore the eigenvector sensitivity coefficients with respect to the change of system

parameter σ are given by

$$\frac{\partial \mathbf{u}_i}{\partial \sigma} = \sum_{j=1,j\neq i}^{N} \frac{\mathbf{v}_j^T(\frac{\partial \mathbf{A}}{\partial \sigma})\mathbf{u}_i}{\lambda_i - \lambda_j} \mathbf{u}_j \quad (i = 1,2,...,N) \tag{5.32}$$

$$\frac{\partial \mathbf{v}_j^T}{\partial \sigma} = - \sum_{i=1,i\neq j}^{N} \frac{\mathbf{v}_j^T(\frac{\partial \mathbf{A}}{\partial \sigma})\mathbf{u}_i}{\lambda_i - \lambda_j} \mathbf{v}_i^T \quad (j = 1,2,...,N) \tag{5.33}$$

5.3   Sensitivity of the Normal Form Transformation

The normal form transformation (4.16) provides the second order terms in the system

and its coefficient is given by

$$h2_{kl}^j = \frac{C_{kl}^j}{\lambda_k + \lambda_l - \lambda_j} \quad (j,k,l = 1,2,...,N) \tag{5.34}$$

Using equation (5.34) we obtain for its sensitivity with respect to the exciter parameter σ as follows.

$$\frac{\partial h2_{kl}^j}{\partial \sigma} = \frac{\frac{\partial C_{kl}^j}{\partial \sigma}(\lambda_k + \lambda_l - \lambda_j) - C_{kl}^j(\frac{\partial \lambda_k}{\partial \sigma} + \frac{\partial \lambda_l}{\partial \sigma} - \frac{\partial \lambda_j}{\partial \sigma})}{(\lambda_k + \lambda_l - \lambda_j)^2} \quad (j,k,l = 1,2,...,N) \tag{5.35}$$

where,

$$\frac{\partial C_{kl}^j}{\partial \sigma} = \frac{1}{2} \sum_{p=1}^{N} \frac{\partial V_{jp}^T}{\partial \sigma} U^T H^p U + V_{jp}^T \frac{\partial U^T}{\partial \sigma} H^p U + V_{jp}^T U^T H^p \frac{\partial U}{\partial \sigma}$$

This consists of eigenvalue sensitivity (5.10) and eigenvector sensitivity (5.32) and (5.33) which were developed in the previous sections. These sensitivity quantities will be used in the sequel to analyze the dependence of the behavior of the critical modes on varying exciter parameter settings.

6 PROPOSED CONTROL TUNING PROCEDURE

In the previous chapters several measures of system performance are presented. These will be applied to tune the control to obtain better system performance. The systematic procedure for the control tuning is presented here.

6.1 A. Determination of Critical Modes

At first the critical modes need to be identified. The critical modes include the inertial modes which are the poorly damped, low frequency interarea modes with high nonlinearity and the control modes which represent the effect of the controllers on the system. These are determined as follows:

1. Data preparation: In order to develop the system equations at the post disturbance equilibrium point, the following data are needed:

   - Power flow study of the prefault network to determine the bus data such as voltage, generation power etc.

   - Dynamic data of generators and controllers

   - Network reduction data (Reduced Y bus matrix)

   - Disturbance simulation: The type and location of disturbance, time of switchings, and the maximum simulation time need to be specified.

2. Build system equations (3.16) as described in Chapter 3 and determine the equilibrium points x_{ep} which are the the real roots of the equation (4.1).

3. Perform eigenanalysis on the system equations to calculate eigenvalues, left and right eigenvectors, and linear participation factors (4.35).

4. Determine whether the system is stable or not.

   - Stable case: Identify the poorly damped low frequency interarea modes and control modes using linear participation factors.

   - Unstable case: In order to find a stable equilibrium point, we need to change the controller setting. Eigenvalue sensitivity (5.10) provides the information for finding the control law. If this sensitivity is positive (negative), adjust the corresponding gain setting to lower (higher) values to obtain a stable system. Then go back to step A.2 with different controller setting.

5. Perform normal form calculations to get the Hessian matrix, h2 coefficients (4.16), and obtain the initial conditions, x_o, y_o, and z_o (see Appendix A.1 for details).

6. Calculate the nonlinear interaction index (I1) (4.30). The size of these measures provides the degree of modal interaction at each mode. This is used to identify the mode with the dominant modal interaction. Most of control modes have large nonlinear interaction index values since they are interacting with the other modes strongly. Therefore we could find the critical inertial modes which can influence system dynamic performance considerably among non-control modes.

7. Calculate 2nd order interaction coefficients (4.34) at the critical modes in order to find the control modes with modal interactions with those modes. Also, we need to apply this step to the control modes which have the modal interactions with the critical modes to find the indirect interactions with the critical modes.

8. Find the controllers which participate in the modal interaction (combination mode) at the critical inertial modes and control modes. The nonlinear participation

factors (4.37) can be used to identify the control states which can control the combination modes.

6.2 B. Control Tuning Procedure

The detailed control tuning procedure based on the results of step A is presented in this section.

1. Compute the sensitivity of the normal form coefficients of the identified critical inertial modes with respect to the control parameter of the controller. The sensitivity value determines the influence of the parameter changes on the nonlinear behavior of system, hence it provides a guide to control tuning to reduce the nonlinear modal interactions at the critical inertial modes. At first we need to determine the combination modes which have large sensitivity values and strong interactions with the critical inertial modes. We then need to identify the control states to be controlled using nonlinear participation factors .

2. For the selected control states identified in the previous step, find an appropriate control law to reduce the nonlinearity of the critical inertial modes based on the sensitivity of the eigenvalues and normal form coefficients.

3. Among different controller settings that result in similar stability behavior of the critical inertial modes, choose the one with lower nonlinearity index (I2) for the critical inertial modes. The index I2 is a measure of the relative size of the nonlinearity in the initial value and represents the normalized severity by nonlinear interaction and is used to find the optimal case among several cases.

Figure 6.1 shows the flow chart of proposed control tuning procedure.

The procedure proposed is tested on the model of a realistic stressed power system and the numerical results are presented in chapter 7.
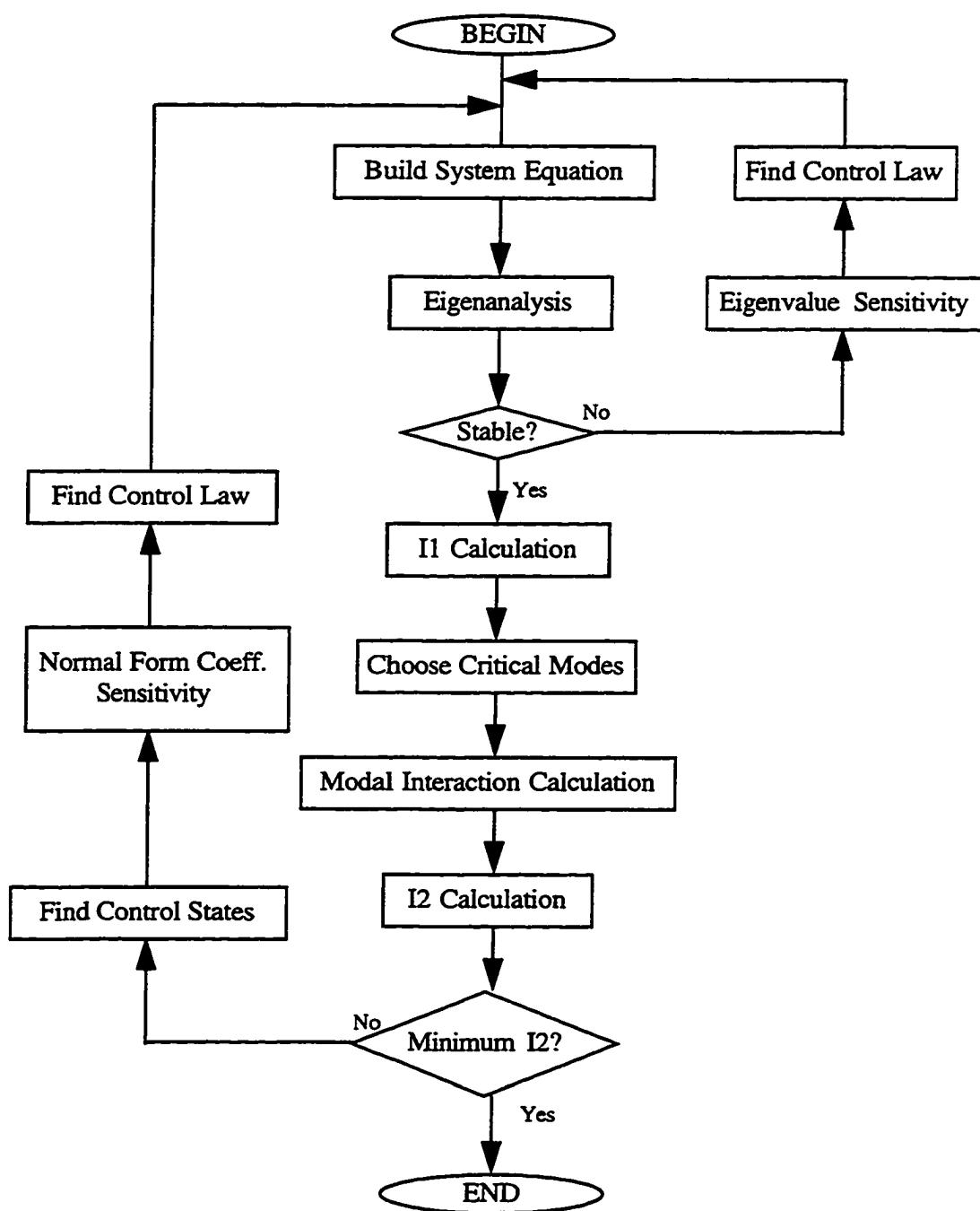
Figure 6.1 Flow chart for control tuning

7 NUMERICAL RESULTS

7.1 The Test System

The 50-generator, 145-bus system is used to provide the numerical results, and this system demonstrates a wide range of dynamic characteristics at different loading levels [32]. Figure 7.1 shows the major part of the 50-generator system.

In our case six machines are represented by the two-axis model and equipped with exciters and the others are represented by the classical model. The exciter data for these six generators is given in Table 7.1. The machine data is given in Table 7.2 on a 100 MVA base and the six generators with the two-axis representation are placed at the top of the table. The power flow bus data is presented in Appendix B.

Table 7.1   50-generator system exciter data

Bus Number	K_A	τ_A	τ_C	τ_B	τ_R	$E_{FD_{max}}$	$E_{FD_{min}}$
93	120	0.020	1.0	10.0	0.01	8.89	-2.0
104	200	0.015	1.0	10.0	0.01	8.86	-7.0
105	50	0.468	1.0	10.0	0.01	7.38	-0.0
106	50	0.468	1.0	10.0	0.01	7.38	-0.0
110	120	0.020	1.0	10.0	0.01	8.89	-2.0
111	200	0.015	1.0	10.0	0.01	8.86	-7.0
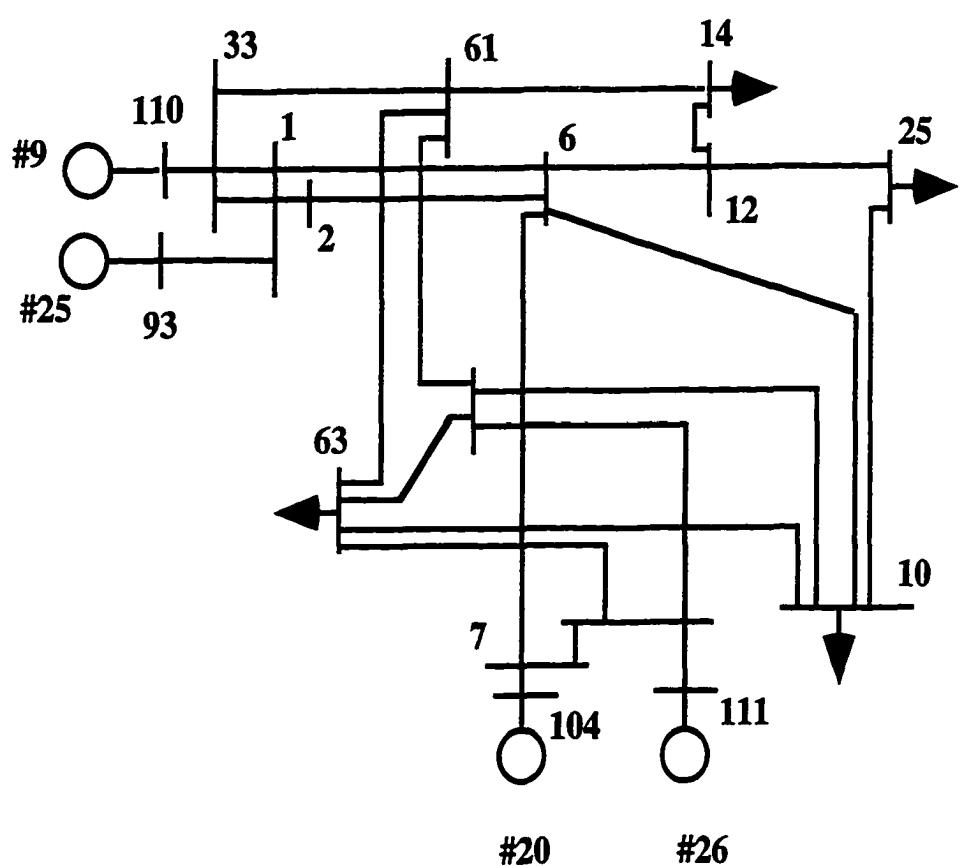
Figure 7.1   The study area of 50-generator system

Table 7.2   50-generator system machine data

Machine #	Bus #	H(s)	$x'_d(pu)$	$x'_q(pu)$	$x_d(pu)$	$x_q(pu)$	$x_l(pu)$	$\tau'_{do}(s)$	$\tau'_{qo}(s)$
1	93	115.04	0.0240	0.03655	0.09842	0.09673	0.01237	8.50	1.24
2	104	73.85	0.0122	0.01440	0.10160	0.09820	0.00810	10.00	1.50
3	105	84.39	0.0208	0.03149	0.11440	0.10920	0.01102	6.61	1.50
4	106	56.26	0.0312	0.04720	0.17165	0.16377	0.01653	6.61	1.50
5	110	115.05	0.0240	0.03655	0.09842	0.09673	0.01237	8.50	1.24
6	111	73.85	0.0122	0.01440	0.10160	0.09820	0.00810	10.00	1.50
7	60	1.41	0.4769						
8	67	52.18	0.0213						
9	79	6.65	0.1292						
10	80	1.29	0.6648						
11	82	2.12	0.5291						
12	89	20.56	0.0585						
13	90	0.76	1.6000						
14	91	1.68	0.3718						
15	94	17.34	0.0839						
16	95	5.47	0.1619						
17	96	2.12	0.4824						
18	97	5.49	0.2125						
19	98	13.96	0.0795						
20	99	17.11	0.1146						
21	100	7.56	0.1386						
22	101	12.28	0.0924						
23	102	78.44	0.0135						
24	103	8.16	0.1063						
25	108	30.43	0.0248						
26	109	2.66	0.2029						
27	112	12.28	0.0924						
28	115	97.33	0.0024						
29	116	105.50	0.0022						
30	117	102.16	0.0017						
31	118	162.74	0.0014						
32	119	348.22	0.0002						
33	121	116.54	0.0017						
34	122	39.24	0.0089						
35	124	116.86	0.0017						
36	128	503.87	0.0001						
37	130	230.90	0.0010						
38	131	1101.72	0.0001						
39	132	120.35	0.0016						
40	134	802.12	0.0003						
41	135	232.63	0.0008						
42	136	2018.17	0.0001						
43	137	469.32	0.0004						
44	139	2210.20	0.0001						
45	140	899.19	0.0003						
46	141	1474.22	0.0001						
47	142	950.80	0.0003						
48	143	204.30	0.0023						
49	144	443.22	0.0004						
50	145	518.08	0.0018						

7.2 Base Case Study (Case I): Ka(Bus #104 & 111) = 200, Ka(Bus #105 & 106) = 50

In this section we apply the proposed control tuning procedure to the test system described in the previous section. The base case with the exciter setting of Table 7.1 is analyzed and its result is presented here.

7.2.1 Linear Analysis

Eigenanalysis on the base case gives eigenvalues, eigenvectors, and linear participation factors. The information of linear participation factors identifies two low frequency inertial modes among poorly damped modes, namely modes 95 and 97. The eigenvalues of these modes are given in Table 7.3 (and all of the eigenvalues are given in Table 7.4).

Table 7.3 Eigenvalues of low frequency modes: Case 1

Low frequency inertial mode	Eigenvalues
95	$-0.00329 \pm j2.05431$
97	$-0.00251 \pm j1.89205$

We will concentrate on these modes and their interaction with control modes throughout this section. Table 7.5 shows the states participating in the important modes. We classify the states into two groups; machine and exciter states. The 'xe..' followed by machine number represents exciter states which are $E_{FD..}$, $x_{E1..}$ or $x_{E2..}$ of the machine, and the others are machine states which are represented by 'x..'. The machine number is given in Table 7.1.

From Table 7.5 we see that mode 95/96 is an interarea mode since the states which participate in this mode belong to generators electrically far away from each other. Modes 101/102 and 103/104 are control modes since their dominant participating states are exciter states, and mode 101/102 is the control mode dominated by the Bus #105 & 106 exciters and mode 103/104 is dominated by the Bus #104 & 111 exciters. The

Table 7.4 Eigenvalues (rad/sec) for Case 1

Mode	Eigenvalue	Mode	Eigenvalue	Mode	Eigenvalue
1	$-0.011 + j19.041$	44	$-0.026 - j9.991$	87	$-0.002 + j3.967$
2	$-0.011 - j19.041$	45	$-0.015 + j9.623$	88	$-0.002 - j3.967$
3	$-0.861 + j18.089$	46	$-0.015 - j9.623$	89	$-0.003 + j3.684$
4	$-0.861 - j18.089$	47	$-0.126 + j9.291$	90	$-0.003 - j3.684$
5	$-0.013 + j15.831$	48	$-0.126 - j9.291$	91	$-0.010 + j3.026$
6	$-0.013 - j15.831$	49	$-0.075 + j9.087$	92	$-0.010 - j3.026$
7	$-0.018 + j15.235$	50	$-0.075 - j9.087$	93	$-0.008 + j2.817$
8	$-0.018 - j15.235$	51	$-0.013 + j8.664$	94	$-0.008 - j2.817$
9	$-0.739 + j14.303$	52	$-0.013 - j8.664$	95	$-0.003 + j2.054$
10	$-0.739 - j14.303$	53	$-0.102 + j8.364$	96	$-0.003 - j2.054$
11	$-0.837 + j14.364$	54	$-0.102 - j8.364$	97	$-0.003 + j1.892$
12	$-0.837 - j14.364$	55	$-0.211 + j8.395$	98	$-0.003 - j1.892$
13	$-0.010 + j13.435$	56	$-0.211 - j8.395$	99	$-1.952 + j0.140$
14	$-0.010 - j13.435$	57	$-0.356 + j8.164$	100	$-1.952 - j0.140$
15	$-0.505 + j12.936$	58	$-0.356 - j8.164$	101	$-1.779 + j0.075$
16	$-0.505 - j12.936$	59	$-0.028 + j8.221$	102	$-1.779 - j0.075$
17	$-0.037 + j12.317$	60	$-0.028 - j8.221$	103	$-0.702 + j0.928$
18	$-0.037 - j12.317$	61	$-0.121 + j8.037$	104	$-0.702 - j0.928$
19	$-0.042 + j11.809$	62	$-0.121 - j8.037$	105	$-0.443 + j0.632$
20	$-0.042 - j11.809$	63	$-0.075 + j8.045$	106	$-0.443 - j0.632$
21	$-0.102 + j11.708$	64	$-0.075 - j8.045$	107	$-0.381 + j0.583$
22	$-0.102 - j11.708$	65	$-0.515 + j7.346$	108	$-0.381 - j0.583$
23	$-0.009 + j11.347$	66	$-0.515 - j7.346$	109	$-0.227 + j0.517$
24	$-0.009 - j11.347$	67	$-0.002 + j7.695$	110	$-0.227 - j0.517$
25	$-1.563 + j9.965$	68	$-0.002 - j7.695$	111	$-0.295 + j0.403$
26	$-1.563 - j9.965$	69	$-0.171 + j7.477$	112	$-0.295 - j0.403$
27	$-0.126 + j10.948$	70	$-0.171 - j7.477$	113	$-0.200 + j0.396$
28	$-0.126 - j10.948$	71	$-0.022 + j7.270$	114	$-0.200 - j0.396$
29	$-0.161 + j10.951$	72	$-0.022 - j7.270$	115	-0.010
30	$-0.161 - j10.951$	73	$-0.057 + j7.148$	116	-1.315
31	$-0.014 + j10.580$	74	$-0.057 - j7.148$	117	-1.461
32	$-0.014 - j10.580$	75	$-0.014 + j7.054$	118	-2.274
33	$-0.200 + j10.650$	76	$-0.014 - j7.054$	119	-2.889
34	$-0.200 - j10.650$	77	$-0.050 + j6.697$	120	-100.004
35	$-0.581 + j10.444$	78	$-0.050 - j6.697$	121	-48.630
36	$-0.581 - j10.444$	79	$-0.200 + j6.274$	122	-100.006
37	$-0.500 + j10.573$	80	$-0.200 - j6.274$	123	-49.318
38	$-0.500 - j10.573$	81	$-0.033 + j5.219$	124	-100.340
39	$-0.327 + j10.534$	82	$-0.033 - j5.219$	125	-100.658
40	$-0.327 - j10.534$	83	$-0.141 + j5.120$	126	-101.106
41	$-0.356 + j10.520$	84	$-0.141 - j5.120$	127	-101.666
42	$-0.356 - j10.520$	85	$-0.006 + j4.769$	128	-64.974
43	$-0.026 + j9.991$	86	$-0.006 - j4.769$	129	-64.122

Table 7.5   Participating states: Case 1

Mode	Participating states
95	x50,x44,x43,x42,x48,x36,x38,x40,x5,x1
97	x43,x50,x44,x42,x36
101	xe3,x3,xe4,x4
103	xe2,x2,xe6,x6,xe1
116	x5,x1,x3,xe5,xe1,x4,xe2

control mode 116 shows participating states from both exciters. It is important to notice that modes 95 and 97 show no substantial participation of exciter states, and that modes 101, 103, and 116 have no participation of the inertial modes 95 and 97. Therefore, on this level of linear analysis it is not possible to predict the influence of the control settings on the important inertial modes. In order to understand, how the exciter gains influence the eigenvalues of modes 95 and 97, we compute their eigenvalue sensitivity with respect to Ka (Bus #104 & 111) and Ka (Bus #105 & 106). The results are shown in Table 7.6. The linear sensitivity analysis indicates that the real part of mode 95 is affected more by the gain settings of the exciters at Bus #104 & 111 than Bus #105 & 106 as seen by the higher value of the eigenvalue sensitivity. Increasing the gain will push the eigenvalue into the right half plane.

Table 7.6   Eigenvalue sensitivity: Case 1

Mode	Ka of Bus #104&111	Ka of Bus #105&106
95	0.966e-4+j0.728e-4	0.709e-4-j0.908e-4
97	0.295e-4+j0.279e-4	0.271e-4-j0.297e-4

7.2.2   Observation of Eigenvalue Sensitivity

We express the dependence of the eigenvalues on Ka (Bus #104 & 111) and Ka (Bus #105 & 106) as a linear function, using the values from Tables 7.3 and 7.6. This corresponds to the first order term in the Taylor expansion of the eigenvalues as functions of Ka. We obtain for the real part of mode 95 as a function of Ka (Bus #104 & 111) :

Table 7.7 Eigenvalue dependence of modes 95&97: Case1

Ka		linear sensitivity		full system	
		mode 95	mode 97	mode 95	mode 97
200	50	-0.003289	-0.002513	-0.003289	-0.002513
180	50	-0.005221	-0.003103	-0.005344	-0.003169
200	45	-0.003646	-0.002646	-0.003636	-0.002644
240	50	0.000572	-0.001334	0.000046	-0.001594
200	60	-0.002582	-0.002239	-0.002545	-0.002224

$$\lambda_N = 0.0000966 * Ka - 0.02260$$

and as a function of Ka (Bus #105 & 106):

$$\lambda_P = 0.0000709 * Ka - 0.006836$$

Table 7.7 shows some values of these functions, and the true values obtained from the analysis of the nonlinear system with corresponding gain settings.

On the level of linear sensitivity of the real parts of the eigenvalue it can be seen that mode 95 is more sensitive to exciter gain changes than mode 97. The influence of both exciters is of similar magnitude in both modes. From these data it is not clear, via which mechanism the exciters influence the critical inertial modes, nor is it clear, which exciters have dominant influence. A comparison of Figures 7.2 and 7.3 shows that the real parts of the eigenvalues of mode 95 depend as concave functions on Ka (Bus #104 & 111), hence the linear analysis underestimates the stability reserve of the system, while they depend as convex functions on Ka (Bus #105 & 106), i.e., the linear analysis overestimates the stability reserve in this case. The following analysis based on 2nd order normal forms will explain these phenomena.

7.2.3 Nonlinear Analysis

The nonlinear interaction index I1 (4.30) for the important inertial and control modes is given in Table 7.8. Modes 95 and 97 are identified as the critical low frequency modes
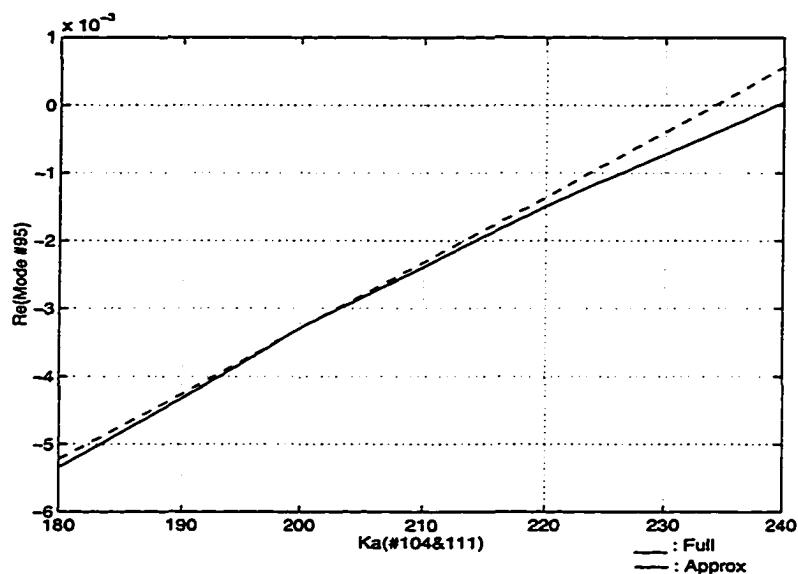
Figure 7.2   Re(λ_{95}) vs. Ka (Bus #104&111)
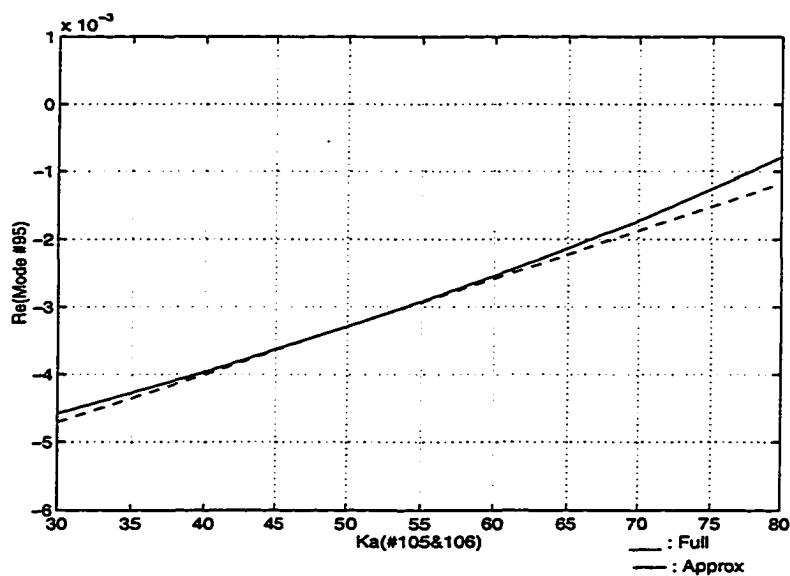
Figure 7.3   Re(λ_{95}) vs. Ka (Bus #105&106)

Table 7.8   Nonlinear interaction index I1: Case 1

Mode	Nonlinear interaction index I1	Rank
95	4.361	13 (2)
97	4.410	11 (1)
101	12.128	7
103	12.297	5

(rank 1 and 2 among these modes), and modes 103 and 101 are the important control modes with participating states dominated by the respective exciters at Bus #104 & 111, and Bus #105 & 106.

The 2nd order interaction coefficients identify those modes that contribute most to the nonlinear (2nd order) solution of the critical modes (4.20). These solutions consist of two terms, the first shows the (nonlinear) dependence on the initial value z_o, the second term account for the nonlinear interaction $h2 * z_o * z_o$. The corresponding values are presented in Table 7.9.

Table 7.9 z_{jo} and 2nd order interactions: Case 1

Mode	z_{jo}	$h2_{kl}^j * z_{ko} * z_{lo}$	
95	0.211 $\angle$-141.0	(116,116)	3.68$\angle$33.6
		(101,102)	2.83$\angle$37.1
		(101,116)	1.64$\angle$-45.6
		(103,104)	0.92$\angle$-165.1
97	1.801 $\angle$101.9	(116,116)	2.57$\angle$-94.7
		(101,102)	1.97$\angle$-91.9
		(81,82)	1.40$\angle$34.9
		(103,104)	0.67$\angle$68.7
101	11.812 $\angle$178.7	(103,104)	4.98$\angle$36.9
		(101,115)	3.09$\angle$-77.9
		(116,116)	3.06$\angle$27.2
103	7.205 $\angle$-57.6	(103,115)	4.95$\angle$-97.4
		(97,104)	3.03$\angle$146.4
		(103,104)	2.04$\angle$-126.3
116	7.788 $\angle$0.0	(103,104)	7.36$\angle$0.0
		(115,116)	0.62$\angle$0.0
		(116,116)	0.60$\angle$0.0

This Table 7.9 identifies the control mode 116 as the dominant interaction mode for both inertial modes, followed by the control modes 101 and 103. In order to assess the influence of the exciter gains on the behavior of the inertial modes 95 and 97, we look at the participation factors and at the sensitivity of the normal form transformation with respect to exciter gains.

Linear participation analysis (Table 7.5) shows that mode 101/102 is dominated by the exciters at Bus #105 & 106, mode 103/104 by the exciters at Bus #104 & 111, and mode 116 shows participation from both inertial and control modes. The nonlinear 2nd order participating states (4.37) are given in Table 7.10.

Table 7.10 Nonlinear participating states: Case 1

Interacting combination mode	Participating states
(116,116)	xe2,xe6
(101,102)	xe2,xe3,xe6,xe4
(103,104)	xe1,xe6,xe5,xe2

The interaction mode (116,116) is dominated by the exciters at Bus #104 & 111, and even the modes (101,102) and (103,104) show substantial influence of the same exciters. This indicates that gain variation at the exciters at Bus #104 & 111 will have the greatest influence on the systems nonlinear behavior. This agrees with the (linear) eigenvalue sensitivity reported in Table 7.6.

Sensitivity of the normal form coefficient (5.35) indicates, how fast and in which direction the nonlinearity in the system changes depending on exciter gain variation. Table 7.11 contains the sensitivities of the 2nd order coefficients of the inertial modes with respect to gain variation at Bus #104 & 111 (Ka2) and Bus #105 & 106 (Ka3).

Table 7.11 shows that both inertial modes have the largest sensitivity values at the combination (or interacting) mode (103, 104) and both are more sensitive to the variation of the exciter gain at Ka2 (Bus #104 & 111). The interacting modes that are predominantly affected by the change of Ka2 all contain participating states of the

Table 7.11　Sensitivity of the 2nd order normal form coefficients: Case 1

Mode j	Modes (k,l)		$\partial h^j_{kl}/\partial Ka$	
			Rectangular Form	Polar Form
95	(103,104)	Ka2	0.78e+0+j0.85e+0	0.12e+1∠47.4
		Ka3	-0.48e+0-j0.92e-1	0.49e+0∠190.9
	(104,118)	Ka2	-0.21e-2+j0.41e-1	0.41e-1∠92.9
		Ka3	-0.13e-1+j0.11e-2	0.13e-1∠175.1
	(103,118)	Ka2	-0.51e-1+j0.53e-1	0.73e-1∠133.9
		Ka3	0.58e-2+j0.22e-1	0.22e-1∠74.8
	(116,116)	Ka2	-0.17e-4-j0.22e-4	0.28e-4∠231.7
		Ka3	0.11e-4-j0.30e-4	0.32e-4∠-69.5
	(101,102)	Ka2	-0.50e-4-j0.58e-4	0.77e-4∠229.2
		Ka3	0.21e-2-j0.28e-2	0.35e-2∠-54.1
	(101,116)	Ka2	-0.33e-4+j0.36e-4	0.49e-4∠132.5
		Ka3	0.92e-3-j0.17e-2	0.19e-2∠-61.4
97	(103,104)	Ka2	0.48e+0+j0.92e+0	0.10e+1∠62.4
		Ka3	0.16e-1+j0.32e-1	0.36e-1∠63.9
	(103,118)	Ka2	-0.59e-1+j0.48e-1	0.75e-1∠140.8
		Ka3	0.83e-2+j0.25e-1	0.26e-1∠71.4
	(116,116)	Ka2	0.12e-5-j0.19e-4	0.19e-4∠-86.6
		Ka3	0.18e-4-j0.34e-4	0.38e-4∠-61.4
	(101,102)	Ka2	0.18e-4-j0.64e-4	0.66e-4∠-74.7
		Ka3	0.25e-2-j0.37e-2	0.45e-2∠-55.4
	(81,82)	Ka2	-0.36e-3-j0.56e-3	0.66e-3∠237.4
		Ka3	-0.59e-3+j0.66e-3	0.88e-3∠132.0

exciters at Bus #104 & 111, hence increasing the gain Ka2 will lead to an increase in the nonlinear behavior of the system as shown by the results of Table 7.7, and 7.11. In addition we also note that the linear sensitivity analysis does not correctly capture the change in stability behavior for the change in exciter settings because of the nonlinearity caused by the change. As a result, these cases illustrates the importance of using the normal forms analysis to include the effects of the nonlinearity.

7.3 Case Studies

According to the results of the base case, increasing the gain Ka2 (Bus #104 & 111) will cause an increase in the nonlinear behavior of the system. This suggests the next case which has the reduced gain Ka2 (Bus #104 & 111).

7.3.1 Case II : Ka(Bus #104 & 111) = 180, Ka(Bus #105 & 106) = 50

Linear analysis (Table 7.12 and 7.13) indicates that mode 95 and 97 are the critical inertial modes of oscillation and the system is more stable than Case I as we expected from the results of eigenvalue sensitivity. For the linear participating states there are no changes to that obtained for Case I.

The linear sensitivity analysis (Table 7.14) indicates that real part of mode 95 is affected more by the gain settings of the exciters at Bus #104 & 111 than at Bus #105 & 106. This also occurred in Case I, but the difference between the values at Bus #104 & 111 and Bus #105 & 106 becomes larger; i.e. compared to Case 1, the sensitivity wrt Ka (Bus #104 & 111) has increased and that wrt Ka (Bus #105 & 106) has decreased.

Table 7.12   Eigenvalues of low frequency modes: Case 2

Low frequency inertial mode	Eigenvalues
95	$-0.00534 \pm j2.05296$
97	$-0.00317 \pm j1.89153$

Table 7.13   Participating states: Case 2

Mode	Participating states
95	x44,x43,x42,x50,x48,x36,x38,x40,x5,x1
97	x43,x50,x44,x42,x36
101	xe3,x3,xe4,x4
103	xe2,x2,xe6,x6,xe5
116	x5,x1,x3,xe5,xe1,x4,x6

Table 7.14   Eigenvalue sensitivity: Case 2

Mode	Ka of Bus #104&111	Ka of Bus #105&106
95	0.109e-3+j0.622e-4	0.697e-4-j0.952e-4
97	0.361e-4+j0.242e-4	0.265e-4-j0.330e-4

Table 7.15   Nonlinear interaction index I1: Case 2

Mode	Nonlinear interaction index I1	Rank
95	4.441	13 (2)
97	5.385	11 (1)
101	9.708	8
103	18.781	4
116	15.389	6

The nonlinear interaction index I1 for the important inertial and control modes is given in Table 7.15 and mode 97 is clearly the largest one among the inertial modes. In Case I we note that mode 97 and 95 are ranked 1 and 2, but have index I1 values which are very close.

The z_o and 2nd order interaction coefficients are given in Table 7.16. The effect of the combination mode (116,116) on mode 95 is decreased and it is interesting that mode 95 has a strong interaction with the modes (87,98). Modes 87 and 98 are the inertial modes. However, from Table 7.17 we can see the nonlinear participating states of this mode include control states of several machines. This means that even though the exciters at Bus #104 & 111 are still dominant with respect to nonlinear modal interactions the degree of dominance is reduced and the pattern of interaction is different.

In order to find the dominant exciter associated with the nonlinear modal interac-

Table 7.16 z_{jo} and 2nd order interactions: Case 2

Mode	z_{jo}	$h2^j_{kl} * z_{ko} * z_{lo}$	
95	0.297 $\angle$-50.1	(87,98)	3.58$\angle$-42.1
		(116,116)	2.20$\angle$122.4
		(95,115)	1.21$\angle$41.4
97	1.609 $\angle$-77.7	(97,115)	3.38$\angle$-166.4
		(116,116)	1.55$\angle$-56.5
		(118,118)	0.52$\angle$-48.5
101	5.751 $\angle$30.5	(101,115)	6.74$\angle$134.0
		(116,116)	1.77$\angle$-71.9
		(101,116)	0.82$\angle$-22.6
103	3.216 $\angle$-50.7	(103,115)	10.22$\angle$-94.6
		(97,104)	0.67$\angle$113.5
		(116,116)	0.63$\angle$118.4
116	5.916 $\angle$0.0	(103,104)	8.92$\angle$0.0
		(115,116)	2.31$\angle$180.0
		(116,116)	0.36$\angle$180.0

Table 7.17   Nonlinear participating states: Case 2

Interacting combination mode	Participating states
(87,98)	xe2,xe6,xe1,xe5,x50,xe3
(116,116)	xe2,xe6,xe5,xe1
(97,115)	xe2,xe6,xe1
(101,115)	xe2,xe6,xe3,xe1
(103,115)	xe6,xe2,xe1,xe5
(103,104)	xe1,xe6,xe5,xe2

tions, we perform sensitivity analysis of the 2nd order normal form coefficients and the results are given in Table 7.18. From Table 7.18 the normal form coefficients corresponding to the interaction with modal combinations (87,98) and (103,104) have large values at both Ka's. We note mode 95 has the larger sensitivity with respect to Ka3 (Bus #105 & 106) for the interaction with modes (87,98). These are the combination modes which have the largest nonlinear interaction with mode 95 as shown in Table 7.16.

This suggests the next case at which the gains of exciters at Bus #105 & 106 is changed (reduced). The gain is reduced because the linear eigenvalue sensitivity in Table 7.14 indicates an improvement in stability with the reduction in gain.

Table 7.18 Sensitivity of the 2nd order normal form coefficients: Case 2

Mode j	Modes (k,l)		$\partial h^j_{kl}/\partial Ka$	
			Rectangular Form	Polar Form
95	(116,116)	Ka2	-0.33e-4+j0.58e-4	0.67e-4∠119.7
		Ka3	-0.44e-4+j0.14e-3	0.15e-3∠107.6
	(87,98)	Ka2	0.15e+1+j0.15e-1	0.15e+1∠0.56
		Ka3	-0.93e+0-j0.22e+1	0.24e+1∠246.9
	(103,104)	Ka2	-0.18e+0+j0.18e+1	0.18e+1∠95.8
		Ka3	0.20e+1+j0.35e+1	0.40e+1∠60.2
	(101,102)	Ka2	-0.80e-2+j0.19e-2	0.83e-2∠166.7
		Ka3	0.76e+0-j0.94e+0	0.12e+1∠-51.2
97	(116,116)	Ka2	0.19e-6-j0.12e-4	0.12e-4∠-89.1
		Ka3	0.14e-4-j0.25e-4	0.29e-4∠-60.5
	(97,115)	Ka2	-0.13e-3-j0.65e-3	0.67e-3∠258.5
		Ka3	0.39e-4+j0.89e-2	0.89e-2∠89.8
	(103,104)	Ka2	0.34e+0+j0.61e+0	0.69e+0∠60.9
		Ka3	-0.41e-3+j0.23e-1	0.23e-1∠91.0
	(101,102)	Ka2	0.17e-2-j0.64e-2	0.67e-2∠-75.0
		Ka3	0.29e+0-j0.42e+0	0.51e+0∠-55.1

7.3.2 Case III: Ka(Bus #104 & 111) = 180, Ka(Bus #105 & 106) = 46

As expected, linear analysis (Table 7.19) indicates that the system becomes more stable. The results of linear sensitivity analysis (Table 7.20) are similar to Case II, and the modes 95&97 are still more sensitive to the exciters at Bus #104 & 111.

The nonlinear interaction index I1 for the important inertial and control modes is given in Table 7.21 and mode 95 becomes the largest one among the inertial modes.

Table 7.19 Eigenvalues of low frequency modes: Case 3

Low frequency inertial mode	Eigenvalues
95	$-0.00562 \pm j2.05334$
97	$-0.00327 \pm j1.89166$

Table 7.20 Eigenvalue sensitivity: Case 3

Mode	Ka of Bus #104&111	Ka of Bus #105&106
95	0.108e-03+j0.613e-04	0.670e-04-j0.943e-04
97	0.359e-04+j0.235e-04	0.250e-04-j0.326e-04

Table 7.21 Nonlinear interaction index I1: Case 3

Mode	Nonlinear interaction index I1	Rank
95	17.099	10 (1)
97	7.132	21 (9)
101	42.931	7
103	10.760	17
116	34.238	9

Table 7.22 z_{jo} and 2nd order interactions: Case 3

Mode	z_{jo}	$h2^j_{kl} * z_{ko} * z_{lo}$	
95	0.495 $\angle 26.7$	(116,116)	17.40$\angle$98.9
		(101,116)	16.45$\angle$-139.1
		(102,116)	16.25$\angle$-13.8
97	7.793 $\angle 7.7$	(116,116)	12.26$\angle$48.7
		(101,116)	11.45$\angle$171.0
		(102,116)	11.30$\angle$-63.8
101	25.370 $\angle 35.8$	(116,116)	23.55$\angle$-156.6
		(101,116)	19.00$\angle$-34.1
		(102,116)	18.58$\angle$85.0
103	4.561 $\angle 54.1$	(102,116)	6.58$\angle$163.0
		(101,116)	6.48$\angle$36.3
		(116,116)	5.01$\angle$-71.1
116	16.704 $\angle 0.0$	(103,104)	17.00$\angle$0.0
		(116,116)	2.87$\angle$180.0
		(65,66)	2.26$\angle$0.0

Also, the values of the index I1 increase except for mode 103.

The z_o and 2nd order interaction coefficients are given in Table 7.22. The effect of combination mode (116,116) on mode 95 is increased and becomes the strongest interaction with the critical inertial modes as in Case I. The reduction of the gains of the exciters at Bus #105 & 106 causes the relative increase of the effects of the exciters at Bus #104 & 111 on the system. Also we observe that mode 116 which is included in the all interactions of the critical inertial modes and control modes in Table 7.22 has strong interaction with modes (103,104). According to Table 7.23, most of the strong interactions have the control states of exciters at Bus #104 & 111.

We now note from Table 7.24 that the normal form coefficients of the inertial modes with respect to the modal combination (103,104) has the highest sensitivity w.r.t. change of gain at Ka2 (Bus #104&111). In addition both the sensitivity of the real part and imaginary part are negative, indicating that an increase in gain will reduce the nonlinearity. We proceed to increase the gain of the exciters at Bus #104&111.

Table 7.23 Nonlinear participating states: Case 3

Interacting combination mode	Participating states
(116,116)	xe2,xe6,xe5,xe1
(101,116)	xe6,xe2,xe5,xe1
(102,116)	xe6,xe2,xe5,xe1

Table 7.24 Sensitivity of the 2nd order normal form coefficients: Case 3

Mode j	Modes (k,l)		$\partial h^j_{kl}/\partial Ka$	
			Rectangular Form	Polar Form
95	(116,116)	Ka2	0.21e-4-j0.34e-4	0.40e-4∠-58.6
		Ka3	0.90e-4-j0.99e-4	0.13e-3∠-47.6
	(101,116)	Ka2	0.21e-3+j0.39e-4	0.21e-3∠10.5
		Ka3	-0.19e-1-j0.21e-1	0.28e-1∠228.4
	(103,104)	Ka2	-0.12e+0-j0.28e+1	0.28e+1∠267.6
		Ka3	-0.51e+0-j0.21e+1	0.22e+1∠256.3
97	(116,116)	Ka2	0.77e-6-j0.11e-4	0.11e-4∠-86.0
		Ka3	0.12e-4-j0.21e-4	0.24e-4∠-60.3
	(101,116)	Ka2	-0.14e-4+j0.11e-4	0.18e-4∠142.4
		Ka3	0.28e-3-j0.21e-2	0.21e-2∠-82.3
	(103,104)	Ka2	-0.97e+0-j0.28e+1	0.29e+1∠250.7
		Ka3	-0.51e-1-j0.88e-1	0.10e+0∠239.9

7.3.3 Case IV: Ka(Bus #104 & 111) = 240, Ka(Bus #105 & 106) = 46

Linear analysis (Table 7.25) shows that the system (mode 95) has less damping than the previous cases. The results of linear sensitivity analysis (Table 7.26) show that the sensitivity of mode 95 to both exciters is similar. From Table 7.27, we observe that mode 95 has the largest index I1 among the inertial modes.

Table 7.25   Eigenvalues of low frequency modes: Case 4

Low frequency inertial mode	Eigenvalues
95	$-0.000235 \pm j2.05784$
97	$-0.001697 \pm j1.89333$

Table 7.26   Eigenvalue sensitivity: Case 4

Mode	Ka of Bus #104&111	Ka of Bus #105&106
95	0.701e-4+j0.846e-4	0.691e-4-j0.819e-4
97	0.170e-4+j0.295e-4	0.253e-4-j0.238e-4

Table 7.27   Nonlinear interaction index I1: Case 4

Mode	Nonlinear interaction index I1	Rank
95	4.380	9 (1)
97	3.567	12 (2)
101	17.114	4
103	19.742	2
116	1.570	17

Table 7.28 z_{jo} and 2nd order interactions: Case 4

Mode	z_{jo}	$h2^j_{kl} * z_{ko} * z_{lo}$	
95	$0.154\angle-4.5$	(87,98)	$2.17\angle-4.6$
		(101,102)	$1.08\angle110.4$
		(102,102)	$0.55\angle12.9$
97	$1.391\angle-73.9$	(97,115)	$1.88\angle-161.1$
		(101,102)	$0.74\angle-106.9$
		(102,102)	$0.38\angle156.4$
101	$7.739\angle-82.6$	(101,115)	$11.85\angle-165.3$
		(103,104)	$7.54\angle-6.8$
		(102,115)	$1.62\angle50.0$
103	$4.504\angle-66.6$	(103,115)	$9.65\angle-97.9$
		(97,104)	$6.23\angle142.6$
		(103,104)	$0.78\angle-135.7$
116	$1.670\angle0.0$	(103,104)	$0.77\angle0.0$
		(115,116)	$0.38\angle0.0$
		(101,104)	$0.18\angle-149.2$

From Table 7.28 and 7.29, we determine that the patterns of nonlinear modal interactions and their participating states are similar to Case 2. Also, we can see from Table 7.29 that the exciter states at Bus #104 & 111 are dominant in these interactions. Table 7.30 shows the normal form coefficient is more sensitive to the variation at Bus #105 & 106 than Bus #104 & 111. In addition, for the most dominant interaction of the critical inertial mode 95 with modal combination (87,98) the sensitivity is highest with respect to Ka3 (Bus #105 & 106) and is negative on both the real and imaginary parts indicating that an increase in gain will reduce the nonlinear interaction. We proceed to the next case in which we increase the gain of the exciters at Bus #105 & 106.

Table 7.29 Nonlinear participating states: Case 4

Interacting combination mode	Participating states
(87,98)	xe2,xe6,xe1,x50,xe5
(101,102)	xe2,xe6,xe3,xe4,xe1,xe5
(103,104)	xe2,xe6,xe1,xe3
(102,102)	xe2,xe6,xe3,xe4,xe1,xe5

Table 7.30 Sensitivity of the 2nd order normal form coefficients: Case 4

Mode j	Modes (k,l)		$\partial h^j_{kl}/\partial Ka$	
			Rectangular Form	Polar Form
95	(87,98)	Ka2	0.92e+0+j0.88e+0	0.13e+1∠43.9
		Ka3	-0.70e+0-j0.20e+1	0.22e+1∠251.2
	(101,102)	Ka2	0.20e-1+j0.17e-1	0.27e-1∠40.6
		Ka3	-0.15e+01-j0.46e+1	0.49e+1∠251.9
	(102,102)	Ka2	-0.28e-1-j0.15e-1	0.32e-1∠207.6
		Ka3	0.58e+1-j0.14e+1	0.59e+1∠-13.5
	(116,116)	Ka2	0.38e-4+j0.62e-4	0.73e-4∠58.3
		Ka3	0.16e-3+j0.17e-3	0.24e-3∠47.3
97	(97,115)	Ka2	-0.36e-4+j0.11e-2	0.11e-2∠91.8
		Ka3	0.28e-1-j0.68e-2	0.29e-1∠-13.7
	(101,102)	Ka2	0.15e-2-j0.46e-2	0.49e-2∠-72.2
		Ka3	0.17e+0-j0.24e+0	0.29e+0∠-55.4
	(102,102)	Ka2	-0.28e-2+j0.98e-2	0.10e-1∠106.1
		Ka3	0.14e+1-j0.10e+1	0.17e+1∠-37.4
	(116,116)	Ka2	0.16e-5-j0.15e-4	0.15e-4∠-84.2
		Ka3	0.11e-4-j0.23e-4	0.25e-4∠-63.7

7.3.4 Case V : Ka(Bus #104 & 111) = 240, Ka(Bus #105 & 106) = 48

For the linear part of the analysis, we again present the eigenvalues and the eigenvalue sensitivities for the important inertial modes 95 and 97, see Tables 7.31, 7.32, and 7.33. Table 7.31 shows the dampings of both modes 96 & 97 are decreased considerably from the base case. The linear sensitivity of the eigenvalues indicates that the change on mode 95 for the change in gain settings is more or less similar.

Table 7.31   Eigenvalues of low frequency modes: Case 5

Low frequency inertial mode	Eigenvalues
95	$-0.00010 \pm j2.05768$
97	$-0.00165 \pm j1.89328$

Table 7.32   Participating states: Case 5

Mode	Participating states
95	x50,x44,x43,x42,x48,x36,x38,x40,x5,x1
97	x43,x50,x44,x42,x36
101	xe3,x3,xe4,x4
103	xe2,x2,xe6,x6,xe1
116	x5,x1,x3,xe5,xe1,x4,xe2

Table 7.33   Eigenvalue sensitivity: Case 5

Mode	Ka of Bus #104&111	Ka of Bus #105&106
95	0.701e-4+j0.850e-4	0.703e-4-j0.822e-4
97	0.169e-5+j0.298e-4	0.259e-4-j0.238e-4

Table 7.34 shows the nonlinearity index I1 for the critical modes, and the index I1 for mode 95 is clearly larger than that for mode 97. Again, from Table 7.35 modal combination (116,116) is the dominant interacting control mode, and this is similar to Case 2 (Table 7.16). We note that we have considerably reduced the magnitude of the nonlinear terms.

Table 7.34   Nonlinear interaction index I1: Case 5

Mode	Nonlinear interaction index I1	Rank
95	1.798	16 (1)
97	1.220	26 (2)
101	7.309	7
103	14.961	3

Table 7.35 z_{jo} and 2nd order interactions: Case 5

Mode	z_{jo}	$h2^j_{kl} * z_{ko} * z_{lo}$	
95	0.141∠-89.3	(87,98)	0.95∠-95.8
		(116,116)	0.81∠23.9
		(103,118)	0.22∠114.0
97	0.983∠175.6	(116,116)	0.56∠-59.2
		(97,115)	0.46∠-91.5
		(103,104)	0.14∠109.9
101	1.641∠148.4	(103,104)	3.71∠117.1
		(116,116)	0.87∠98.7
		(101,115)	0.60∠-110.6
103	3.853∠-48.2	(97,104)	6.50∠-18.4
		(103,115)	2.87∠-79.8
		(103,104)	0.57∠-33.2
116	3.786∠0.0	(103,104)	0.56∠0.0
		(115,116)	0.30∠0.0
		(116,116)	0.13∠0.0

7.4 Finding Optimal Case

The final step in our analysis is to examine the different change cases and determine the nonlinearity index I2. This will provide us a measure of the effect of the control tuning on the nonlinearity introduced and provide a metric for selecting the appropriate setting.

Table 7.36 Eigenvalues and interaction coefficients of mode 95

Case	Ka's		Re(λ)	max(h2zz)	$|z_{jo}|$	I2
I	200	50	-0.00329	3.68	0.211	17.41
II	180	50	-0.00534	3.58	0.297	12.08
III	180	46	-0.00562	17.40	0.495	35.13
IV	240	46	-0.00024	2.17	0.154	14.09
V	240	48	-0.00010	0.95	0.141	6.75

Table 7.37 Eigenvalues and interaction coefficients of mode 97

Case	Ka's		Re(λ)	max(h2zz)	$|z_{jo}|$	I2
I	200	50	-0.00251	2.57	1.801	1.43
II	180	50	-0.00317	3.38	1.609	2.10
III	180	46	-0.00327	12.26	7.793	1.57
IV	240	46	-0.00170	1.88	1.391	1.35
V	240	48	-0.00165	0.56	0.983	0.57

From Tables (7.36 and 7.37) we note that for the inertial modes the index I2 in the last column is lowest for the case where the nonlinearity in the system is the smallest. This corresponds to Case 5 where Ka (Bus #104 & 111) = 240, and Ka (Bus #105 & 106) = 48. This nonlinearity index (I2) compares the magnitude of the largest 2nd order term in comparison to the linear term. The terms used to calculate the index I2 are the coefficients which appear in the closed form solution obtained from the normal form analysis. These terms reflect the inherent structural characteristics of the system. We note that at the setting at which the nonlinear index I2 is the least for the inertial modes, the damping is not the highest. Actually Case 3 has the highest damping. This

design procedure uses the size of the nonlinear term as a criterion for design. It could be refined to include a trade-off between nonlinearity and damping using appropriate weighting factors.

7.5 Time Domain Simulation Results

For nonlinear systems time domain simulation is an important complement to analytical tools in determining whether such specifications are met. Nonlinear time domain simulations are performed for the cases which are analyzed in the previous sections in this section.

7.5.1 Comparison of Stability Margin

We now compare the control settings for Case 1, Case 3 and Case 5 using nonlinear time simulation: For a 3-phase stub fault at Bus #7 cleared at 0.108 second we obtain the stability limit in terms of the plant generation at Bus #93 & 110. We note that Case 1 (Ka of Bus #104 & 111 = 200, Ka of Bus #105 & 106 = 50) and Case 3 (Ka of Bus #104 & 111 = 180, Ka of Bus #105 & 106 = 46) give a limit of 3200 MW and 3170 MW respectively, and Case 5 (Ka of Bus #104 & 111 = 240, Ka of Bus #105 & 106 = 48) provides a limit of 3260 MW at generation of Bus #93 & 110. This clearly indicates the inclusion of the nonlinear effects in the control design provides a higher transient stability limit. The relative angle plots of generator at Bus #93 are shown in Figures 7.4, 7.5, 7.6, and 7.7 according to the total generation of generators at Bus #93 & 110.

From the time simulation results we find the optimal control tuning from the proposed procedure gets better control performance, i.e. the control performance is not affected much by existing nonlinearity.
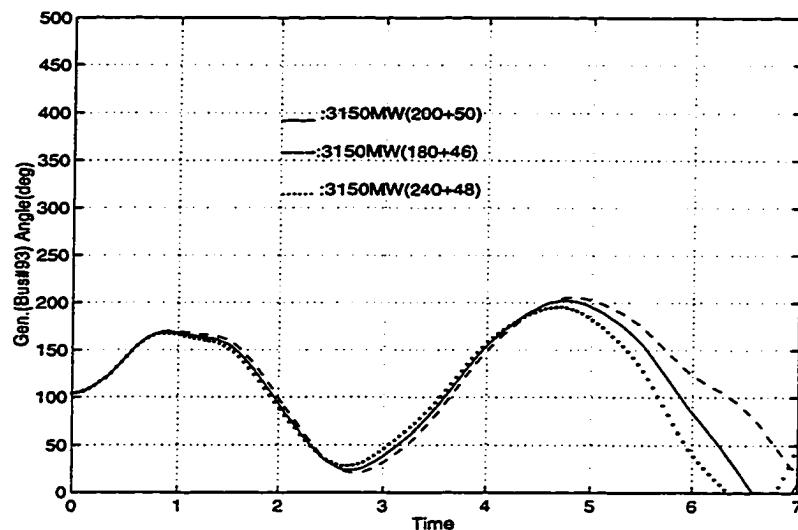
Figure 7.4   Comparison of angle plot of generator at Bus #93 [a]
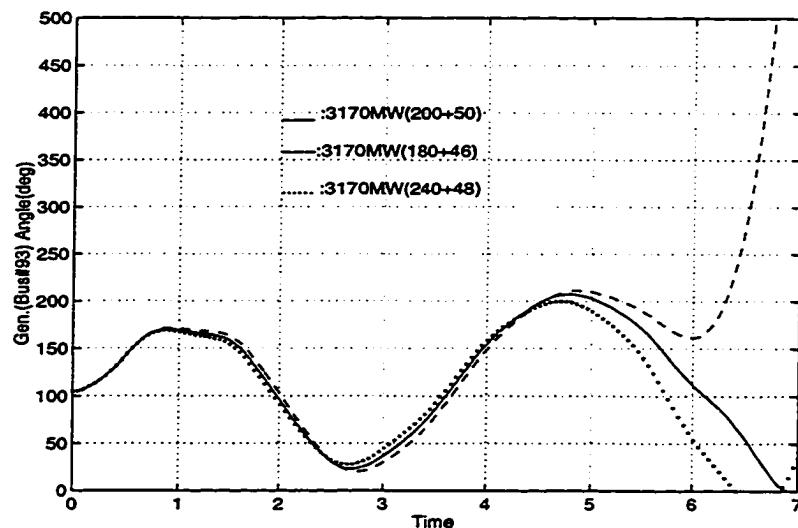
Figure 7.5   Comparison of angle plot of generator at Bus #93 [b]

---

[a]When the total generation at Bus #93 & 110 is 3150MW
[b]When the total generation at Bus #93 & 110 is 3170MW
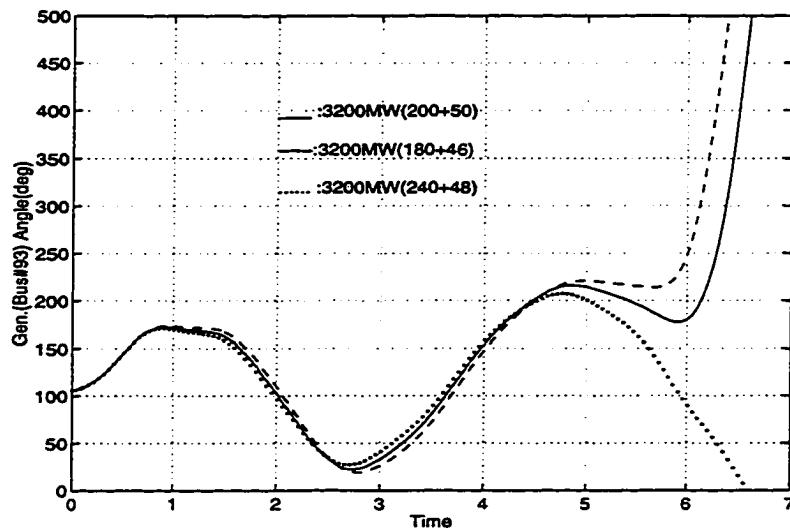
Figure 7.6   Comparison of angle plot of generator at Bus #93 [a]
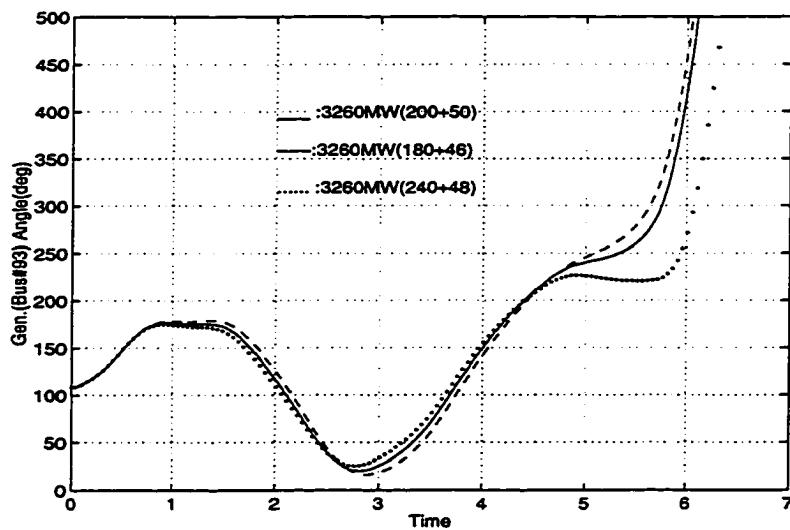
Figure 7.7   Comparison of angle plot of generator at Bus #93 [b]

---

[a]When the total generation at Bus #93 & 110 is 3200MW
[b]When the total generation at Bus #93 & 110 is 3260MW

7.5.2 Effect of Change of Fault Location on Control Tuning

This section deals with the effect of change of fault location on control tuning. This could determine whether the control tuning from the proposed procedure at one fault location is valid for another case in which the fault location is different. In this section, we perform nonlinear time simulation for the case in which the fault occurs at Bus #1 and cleared at 0.108 second, and compare the control settings for Case 1, Case 3, and Case 5 in terms of the plant generation at Bus #93 & 110 as in the previous section. Case 1 (Ka of Bus #104 & 111 = 200, Ka of Bus #105 & 106 = 50) and Case 3 (Ka of Bus #104 & 111 = 180, Ka of Bus #105 & 106 = 46) give a limit of 3320 MW and 3280 MW respectively, and Case 5 (Ka of Bus #104 & 111 = 240, Ka of Bus #105 & 106 = 48) provides a limit of 3340 MW, and the relative angle plots of generator at Bus #93 are shown in Figures 7.8, 7.9, 7.10, and 7.11.

Therefore, we may say the control settings to reduce the nonlinear interaction at the specific fault location could be applied to other cases at different fault locations, even though the initial conditions (x_o, y_o, and z_o) are changed as the location of the disturbance is different.
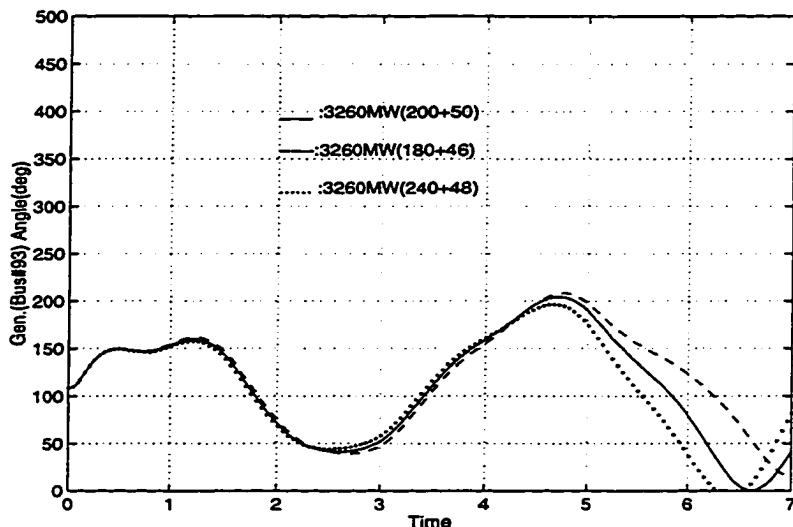
Figure 7.8   Comparison of angle plot of generator at Bus #93 [a]
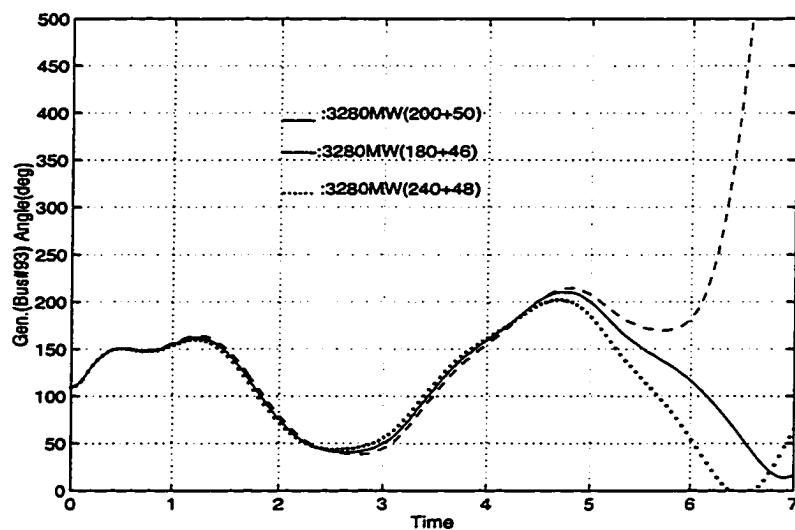
Figure 7.9   Comparison of angle plot of generator at Bus #93 [b]

---

[a]When the total generation at Bus #93 & 110 is 3260MW and fault is at Bus # 1
[b]When the total generation at Bus #93 & 110 is 3280MW and fault is at Bus # 1
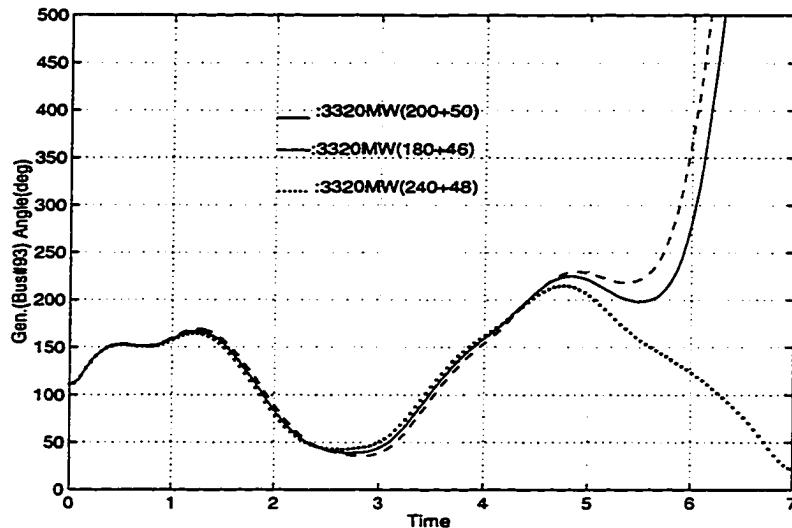
Figure 7.10   Comparison of angle plot of generator at Bus #93 [a]
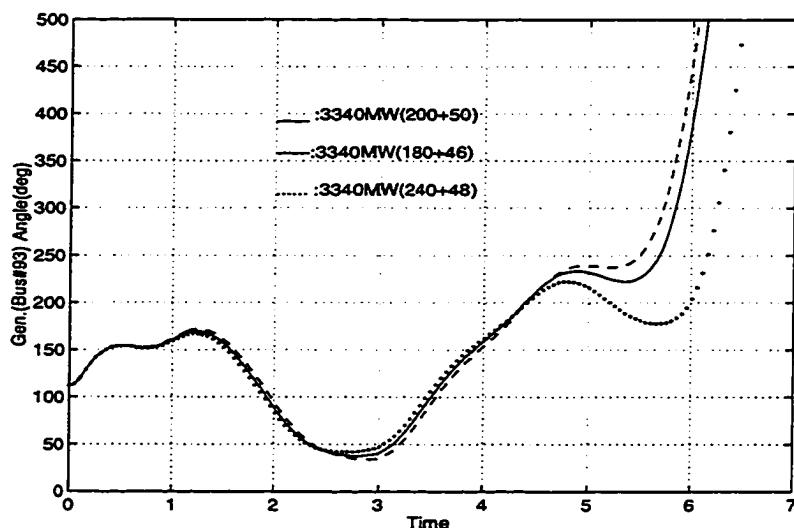
Figure 7.11   Comparison of angle plot of generator at Bus #93 [b]

---

[a]When the total generation at Bus #93 & 110 is 3320MW and fault is at Bus # 1
[b]When the total generation at Bus #93 & 110 is 3340MW and fault is at Bus # 1

8 CONCLUSIONS

This work develops the analytical basis for tuning controls (exciter settings) in power systems using the nonlinear information provided by the method of normal forms. The technique developed is based on using indices to identify control modes which interact nonlinearly with inertial modes. The concept of nonlinear participation factors, and sensitivity of the normal forms coefficient, together with linear participation factors and eigenvalue sensitivity are used to vary control settings. The control settings are varied to obtain improved stability and to reduce the nonlinearity in the system.

The results on a sample test system, demonstrate the importance of including the effect of the second order nonlinear terms in the analysis. The results provided also indicate some of the shortcomings of the linear approach, and illustrate the nature of the added information provided by the higher order terms. The nonlinear interaction index I1 clearly identifies the control modes interacting with the inertial modes, and the use of the nonlinear participation factors provided information regarding the states participating in the interacting modes. The sensitivity of the nonlinear coefficients to the identified control parameters provides information on the changes to the settings to reduce nonlinearity and improve stability.

The results obtained lead to the following conclusions:

- Linear eigenvalue and sensitivity analysis correctly indicate the direction in which exciter gains have to be tuned to stabilize or destabilize a system. They do not indicate, however, how far the exciter gain can be tuned to maintain stability.

- The nonlinear interaction index (I1) accurately identifies the dominant inertial modes and control modes.

- The 2nd order interaction coefficients and nonlinear participating states identify those control modes that influence the nonlinear behavior of the inertial modes.

- Sensitivity of the 2nd order normal form coefficients determines the control parameters that have dominant influence on the stability behavior of the inertial modes. These sensitivities provide a clear indication of control tuning that gives better system performance.

- Changing the exciter gains in a system can change the relative influence of the control settings on the system, compare Case 4 and Case 5. Even quite small changes in one exciter gain can result in another exciter having dominant influence at the resulting control setting.

- The procedure developed accurately identifies the mechanism of control interaction, and allows for changing control settings. These changes are based on a systematic analysis of the structural characteristics of the system.

- The nonlinearity index (I2) identifies the severity of nonlinearity for the stable system and can be used to find optimal setting.

- The inclusion of the nonlinear effects in control design provides a higher transient stability limit.

Based on the experience of this research work. the following suggestions are made for further research work:

- Control tuning procedure using the sensitivity of normal form coefficients is based on system structure. Since system performance depends on system structure and

on initial values, the way to incorporate the sensitivity of initial values needs to be developed for better control tuning.

- For an unstable case where the analysis need to be performed around an Unstable Equilibrium Point (UEP), this work will not always convey the complete picture. This requires a more detailed bifurcation analysis.

- From the view point of numerical analysis the programs which are used for this work have been optimized by eliminating unneeded stores, overlapping operations, and doing operator strength reduction. However the code for this work needs to be improved to reduce the storage memory and calculation speed. It needs about 57 Mbytes for the storage of h2 coefficients, and comparing each run time of whole computation tells the calculation of z_o takes more than 80 % of whole run time. We suggest the parallelization of z_o calculation and the fast calculation of z_o enables main program to incorporate the subroutine for z_o. Then h2 coefficients don't need to be stored separately. In the appendices a sample program for calculation of z_o using a parallelized code is presented.

- Analytical methods for optimal control are suggested to evaluate the stability and nonlinear modal interactions of a system quantitatively and minimize (or maximize) them.

APPENDIX A   DETAILS OF SOLVING z_o

A.1 Procedure for Solving z_o

To determine z_o we need to obtain x_o and y_o and the procedure is as follows:

1. The initial condition $x_o = x_{cl} - x_{SEP}$, where x_{cl} is the system condition at the time of fault clearing and can be obtained by time simulation, and x_{SEP} is defined in chapter 4.

2. Using the transformation $x = Uy$, we get y_o

$$y_o = U^{-1}x_o = V^T x_o \qquad (A.1)$$

where U and V are the matrix of right and left eigenvectors respectively.

3. According to the equation (4.16), the relation between x_o and y_o is

$$y = z + h2(z) \qquad (A.2)$$

where,

$$h2^j(z) = \sum_{k=1}^{N} \sum_{l=1}^{N} h2_{kl}^j z_k z_l \quad (j = 1, 2, ..., N)$$

Therefore, z_o is the solution of following equation.

$$f(z) = -y + z + h2(z) \qquad (A.3)$$

In order to solve the nonlinear equation (A.3), we use a modification of the levenberg-marquardt algorithm and this subroutine is explained in the next section.

A.2 Subroutine for Solving z_o

In order to solve z_o we used a subroutine *lmdif* [33], and the purpose of lmdif is to minimize the sum of the squares of m nonlinear functions in n variables by a modification of the levenberg-marquardt algorithm. For this program we must provide a subroutine which calculates the functions. The Jacobian is then calculated by a forward-difference approximation. The subroutine statement is as follows:

subroutine lmdif(fcn, m, n, x, fvec, ftol, xtol, gtol, maxfev, epsfcn, diag, mode, factor, nprint, info, nfev, fjac, ldfjac, ipvt, qtf, wa1, wa2, wa3, wa4)
where

- *fcn* is the name of the user-supplied subroutine which calculates the functions. fcn must be declared in an external statement in the user calling program, and should be written as follows.

subroutine fcn(m, n, x, fvec, iflag)
integer m, n, iflag
double precision x(n), fvec(m)
calculate the functions at x and return this vector in fvec.
return
end

The value of iflag should not be changed by fcn unless the user wants to terminate execution of lmdif. In this case set iflag to a negative integer.

- *m* is a positive integer input variable set to the number of functions.

- *n* is a positive integer input variable set to the number of variables, and n must not exceed m.

- *x* is an array of length n. On input x must contain an initial estimate of the solution vector. On output x contains the final estimate of the solution vector.

- *fvec* is an output array of length m which contains the functions evaluated at the output x.

- *ftol* is a nonnegative input variable. Termination occurs when both the actual and predicted relative reductions in the sum of squares are at most ftol. Therefore, ftol measures the relative error desired in the sum of squares.

- *xtol* is a nonnegative input variable. Termination occurs when the relative error between two consecutive iterates is at most xtol. Therefore, xtol measures the relative error desired in the approximate solution.

- *gtol* is a nonnegative input variable. Termination occurs when the cosine of the angle between fvec and any column of the Jacobian is at most gtol in absolute value. Therefore, gtol measures the orthogonality desired between the function vector and the columns of the Jacobian.

- *maxfev* is a positive integer input variable. Termination occurs when the number of calls to fcn is at least maxfev by the end of an iteration.

- *epsfcn* is an input variable used in determining a suitable step length for the forward-difference approximation. This approximation assumes that the relative

errors in the functions are of the order of epsfcn. If epsfcn is less than the machine precision, it is assumed that the relative errors in the functions are of the order of the machine precision.

- *diag* is an array of length n. If mode = 1 (see below), diag is internally set. If mode = 2, diag must contain positive entries that serve as multiplicative scale factors for the variables.

- *mode* is an integer input variable. If mode = 1, the variables will be scaled internally. If mode = 2, the scaling is specified by the input diag. Other values of mode are equivalent to mode = 1.

- *factor* is a positive input variable used in determining the initial step bound. This bound is set to the product of factor and the Euclidean norm of diag*x if nonzero, or else to factor itself. In most cases factor should lie in the interval (.1,100.). 100. is a generally recommended value.

- *nprint* is an integer input variable that enables controlled printing of iterates if it is positive. In this case, fcn is called with iflag = 0 at the beginning of the first iteration and every nprint iterations thereafter and immediately prior to return, with x and fvec available for printing. If nprint is not positive, no special calls of fcn with iflag = 0 are made.

- *info* is an integer output variable. If the user has terminated execution, info is set to the (negative) value of iflag. (see description of fcn) Otherwise, info is set as follows.

  - info = 0: improper input parameters.

  - info = 1: both actual and predicted relative reductions in the sum of squares are at most ftol.

– info = 2: relative error between two consecutive iterates is at most xtol.

– info = 3: conditions for info = 1 and info = 2 both hold.

– info = 4: the cosine of the angle between fvec and any column of the Jacobian is at most gtol in absolute value.

– info = 5: number of calls to fcn has reached or exceeded maxfev.

– info = 6: ftol is too small, so no further reduction in the sum of squares is possible.

– info = 7: xtol is too small, so no further improvement in the approximate solution x is possible.

– info = 8: gtol is too small, so fvec is orthogonal to the columns of the Jacobian to machine precision.

- *nfev* is an integer output variable set to the number of calls to fcn.

- *fjac* is an output m by n array. The upper n by n submatrix of fjac contains an upper triangular matrix r with diagonal elements of non-increasing magnitude such that $p^t * (jac^t * jac) * p = r^t * r$ where p is a permutation matrix and jac is the final calculated Jacobian. Column j of p is column ipvt(j) (see below) of the identity matrix. The lower trapezoidal part of fjac contains information generated during the computation of r.

- *ldfjac* is a positive integer input variable not less than m which specifies the leading dimension of the array fjac.

- *ipvt* is an integer output array of length n. ipvt defines a permutation matrix p such that jac*p = q*r, where jac is the final calculated Jacobian, q is orthogonal (not stored), and r is upper triangular with diagonal elements of non-increasing magnitude. Column j of p is column ipvt(j) of the identity matrix.

- *qtf* is an output array of length n which contains the first n elements of the vector (q transpose)*fvec.

- *wa1, wa2,* and *wa3* are work arrays of length n.

- *wa4* is a work array of length m.

A.3 Parallelization of the Code

In this section a sample program which is written by Fortran 77 for parallel computation is presented. MPI (Message Passing Interface) [34] is used to parallelize the code. One approach to parallelizing this program is to simply use the same number of processors as the number of the initial guesses, for example we have 4 general initial guesses to calculate z_o, so with 4 processors we could try those at the same time and reduce the computational time. A sample program to calculate z_o is as follows :

```
program sample

.... Declaration Part
include "mpif.h" ! defines various mpi constants and variables

.... Declaration Part

        call mpi_init(ierr)
c——     Required in every mpi program and must be the first mpi routine called.
c——     ierr is an error code that returns the value mpi_success if this subroutine
c——     successfully completes.

        call mpi_comm_size(mpi_comm_world, nprocs, ierr)
c——     nprocs is the number of processors that have been started up for this program.
        call mpi_comm_rank(mpi_comm_world, rank, ierr)
c——     rank is the number of assigned processor.
```

```
      .... Data Reading Part
c——  h2 coefficients, data from eigenanalysis, x_o, and etc


      call mpi_bcast()
c——  Required data can be used at all processors


      .... Calculation of y_o


      call fcnh2(x,fh2)
c——  This is a subroutine to calculate the summation term of h2


      write(*,*)'There are 4 options to choose the initial guess'
      write(*,*)'1. Zo = 0'
      write(*,*)'2. Zo = Yo'
      write(*,*)'3. Zo = yo-h2(yo)'
      write(*,*)'4. Zo from a file'
      write(*,*)'enter your selection : '
c——  Each initial guess is used at different processors


      If (rank .eq. 0) then
      mpi_send()
      ....
      else


      call lmdif(fcn,ns,ns,x,fvec,ftol,xtol,gtol,maxfev,epsfcn,
      diag,mode,factor,nprint,info,nfev,fjac,ldfjac,
      ipvt,qtf,wa1,wa2,wa3,wa4)
c——  This is a subroutine to calculate z_o


      endif


      call mpi_finalize(ierr)
c——  No mpi functions called after called.


      end
```

APPENDIX B   POWER FLOW GENERATOR BUS DATA

FOR THE TEST SYSTEM

Table B.1   Power flow 50-generator bus data

Bus #	|V| p.u.	ang(V) degree	P_{load} MW	Q_{load} MVAR	P_{gen} MW	Q_{gen} MVAR
60	1.1370	-0.07	0.00	0.00	51.00	30.36
67	1.0900	2.03	0.00	0.00	1486.00	307.22
79	1.0520	-1.22	9.10	3.00	250.20	-17.26
80	1.0690	-.03	17.10	5.00	47.00	-14.62
82	0.9750	-10.25	2.10	1.10	70.00	18.15
89	1.0660	13.17	0.60	0.20	673.00	138.79
90	0.9500	-.45	4.60	1.50	22.00	-4.03
91	1.0000	-0.57	0.00	0.00	64.00	0.30
93	1.0000	10.12	100.40	73.20	900.00	400.92
94	1.0200	5.57	15.40	7.60	300.00	17.11
95	0.9200	23.32	6.70	2.20	131.00	8.13
96	1.0000	0.27	0.00	0.00	60.00	21.56
97	0.9670	3.50	0.00	0.00	140.00	45.61
98	0.9700	14.75	0.00	0.00	426.00	-30.28
99	1.0000	12.56	10.46	5.23	200.00	-4.94
100	1.014	10.20	0.00	0.00	170.00	59.94
101	1.039	3.34	17.80	4.50	310.90	152.08
102	1.019	.51	37.60	9.20	2040.00	511.85
103	1.0000	10.99	0.00	0.00	135.00	5.56
104	1.0045	22.95	30.20	7.60	2000.00	500.00
105	1.0070	6.63	96.00	167.40	1620.00	399.29

Table B.1 (Continued)

106	1.0050	6.67	64.00	16.00	1080.00	217.42
108	1.0140	-6.38	0.00	0.00	800.00	87.25
109	0.9150	-10.02	0.00	0.00	52.00	-14.96
110	1.0000	11.08	100.40	73.20	900.00	547.99
111	1.0000	16.87	60.40	1166.00	2000.00	585.89
112	1.0370	3.16	18.60	4.60	300.00	143.50
115	1.0490	-12.86	683.50	184.70	2493.00	129.86
116	1.0430	-13.22	792.60	315.50	2713.00	634.36
117	1.0300	-10.91	485.30	71.40	2627.00	284.69
118	1.0100	-13.83	651.90	328.40	4220.00	683.90
119	1.0130	-55.03	2094.00	3774.00	8954.00	4774.62
121	1.0460	-13.62	237.70	-17.30	2997.00	-72.65
122	1.0000	3.65	29.20	7.00	1009.00	188.25
124	1.0000	5.48	94.10	780.30	3005.00	607.94
128	1.0250	-34.72	4075.00	703.50	12963.00	2640.14
130	1.0570	-47.95	4328.00	944.30	5937.00	1803.82
131	1.0420	-20.86	21840.00	4320.00	28300.00	7374.55
132	1.0420	-3.14	491.90	110.20	3095.00	646.11
134	1.0440	-9.61	22309.00	7402.00	20626.00	7363.90
135	1.1070	30.76	4298.00	1264.00	5982.00	1565.57
136	1.0830	5.98	52951.00	13552.00	51950.00	1444.09
137	1.0640	-72.22	12946.00	2608.00	12068.00	3449.78
139	1.0400	-9.97	57718.00	13936.00	56834.00	15823.84
140	1.0500	-25.60	24775.00	6676.00	23123.00	6709.95
141	1.0530	-6.94	32799.00	11361.00	37911.00	11607.74
142	1.1550	-7.86	17737.00	3934.00	24449.00	5475.17
143	1.0310	-10.22	4672.00	1709.00	5254.00	2172.34
144	0.9970	-5.72	9602.00	2203.00	11397.00	2682.51
145	1.0520	5.02	9173.00	1555.00	13704.44	2836.85

BIBLIOGRAPHY

[1] Kundur, P., *Power System Stability and Control.* New York: McGraw-Hill Inc.

[2] Koeler, J. E., "Bulk power system voltage phenomena - voltage stability & security," proceedings of voltage stability & security, September 1988. Keynote.

[3] IEEE Power Engineering Society, "Eigenanalysis and frequency domain methods for system dynamic performance," Tech. Rep. 90TH0292-3-PWR, 1989.

[4] Klien, M., G. J. Rogers, and P. Kundur, "A fundamental study of interarea oscillations in power systems," *IEEE Transactions on PWRS*, vol. 6, pp. 914–921, August 1991.

[5] Klien, M., G. J. Rogers, S. Moorty, and P. Kundur, "Analytical investigation of factors influencing power system stabilizers performance." IEEE-PES 1992 Winter Meeting, Paper No. 92 WM 016-6EC.

[6] Vittal, V., N. Bhatia, and A. A. Fouad, "Analysis of the inter-area mode phenomenon in power systems following large disturbances," *IEEE Transactions on PWRS*, vol. 6, pp. 1515–1521, 1991.

[7] Tamura, Y., and N. Yorino, "Possibility of auto-& hetero-parametric resonance in power systems and the relationship to long-term dynamics," *IEEE Transactions on PWRS*, vol. 2, pp. 890–897, Nov. 1987.

[8] Yorino, Y., H. Saski, Y. Tamura, and R. Yokoyama, "A generalized analysis method of auto-parametric resonances in power systems," *IEEE Transactions on PWRS*, vol. 4, pp. 1057–1064, Aug. 1989.

[9] Yoo, Shin-Heng, Hironobu Morita, Yu Huang, and Yasuo Tamura, "On the approximation of the perturbation method to derive the conditions of auto-parametric resonance likely occur in power systems," in *11th PSCC, Avignon France*, pp. 93–305, 1993.

[10] Fouad, A. A., and V. Vittal, *Power System Transient Stability Analysis Using the Transient Energy Function Method*. Englewood Cliffs, New Jersey: Prentice hall Inc., 1992.

[11] Agrawal, B. L., P. M. Anderson, and J. E. Van Ness, *Subsynchronous Resonance in Power Systems*. New York: IEEE Press, 1990.

[12] Hammad, A. E., "Eigenvalue and frequency domain analysis of second harmonic resonance in a complex ac/dc network." IEEE/PES, pp.61-66,90TH0292-3-PWR, 1989.

[13] Pagola, F. L., L. Rouco, and I. J. Perez-Arriaga, "Analysis and control of small signal stability in electric power systems by selective modal analysis." IEEE/PES, pp.77-96,90TH0292-3-PWR, 1989.

[14] Grund, C. E., R. J. O'Keefe, J. J. Paserba, D. L. Carlson, and S. R. Norr, "Development of low-order control design models from standard stability models." IEEE/PES, pp.34-42,90TH0292-3-PWR, 1989.

[15] Arrowsmith, D. K., and C. M. Place, *An Introduction to Dynamical Systems*. Cambridge: Cambridge University Press, 1990.

[16] Arnold, V. I., *Geometrical Methods in the Theory of Ordinary Differential Equations*. New York: Springer-Verlag, 1983.

[17] Ruelle, D., *Elements of Differentiable Dynamics and Bifurcation Theory*. Boston: Academic Press, 1988.

[18] Lin, C., V. Vittal, W. Kliemann, and A. A. Fouad, "Investigation of modal interaction and its effect on control performance in stressed power systems using normal forms of vector fields," *IEEE Transactions on PAS*, vol. 11, pp. 781–787, May 1996.

[19] Saha, S., A. A. Fouad, W. Kliemann, and V. Vittal, "Stability boundary approximation of a power system using the real normal form of vector fields." IEEE/PES Summer Meeting, Paper#96SM503-3, 1996.

[20] Ni, Y., V. Vittal, W. Kliemann, and A. A. Fouad, "Nonlinear modal interaction in hvdc/ac power systems with dc power modulation." IEEE/PES Winter Meeting, Paper#96WM276-6, 1996.

[21] Thapar, J., V. Vittal, W. Kliemann, and A. A. Fouad, "Application of the normal form of vector fields to predict interarea separation in power systems." IEEE/PES Summer Meeting, Paper#96SM517-3, 1996.

[22] Demello, F. P. and C. Concordia, "Concepts of synchronous machine stability as affected by excitation control," *IEEE Transactions on Power Apparatus and Systems*, vol. PAS-88, pp. 316–329, April 1969.

[23] Anderson, P. M., and A. A. Fouad, *Power System Control and Stability*. New York: IEEE Press, 1994.

[24] IEEE Committee Report, "Excitation system models for power system stability studies," *IEEE Transactions on Power Apparatus and Systems*, vol. PAS-100, pp. 494–509, Feb. 1981.

[25] Wiggins, S., *Introduction to Applied Nonlinear Dynamical Systems and Chaos*. New York: Springer-Verlag, 1990.

[26] Luenberger, D. G., *Introduction to Dynamic Systems*. John Wiley & Sons, 1979.

[27] Thapar, J., "Application of normal form of vector fields to predict interarea split following large disturbances in power systems," M.S. Thesis, Iowa State University, Ames, Iowa, 1996.

[28] Perez-Arriaga, I. J., G. C. Verghese, and F. C. Schweppe, "Selective modal analysis with applications to electric power systems. part 1: Heuristic introduction," *IEEE Transactions on PAS*, vol. 101, pp. 3117–3125, Sept. 1982.

[29] Starrett, S. K., "Application of normal forms of vector fields to stressed power systems," Ph.D. Thesis, Iowa State University, Ames, Iowa, 1994.

[30] Crossley, T. R. and B. Porter, "Eigenvalue and eigenvector sensitivities in linear systems theory," *Int. J. Control*, vol. 10, pp. 163–170, 1969.

[31] Porter, B., "Eigenvalue sensitivity of modal control systems to loop-gain variations," *Int. J. Control*, vol. 10, pp. 159–162, 1969.

[32] Vittal, V., "Transient stability test systems for direct stability method," *IEEE Transactions on PAS*, pp. 37–42, Feb. 1992.

[33] "Nonlinear equation solver (minpack)." <http://www.netlib.org>, undated (Accessed 10 Apr. 1996).

[34] Pacheco, P., *A User's Guide to MPI*. San Francisco, CA: University of San Francisco, 1995.